IMMUNOLOGY

TRIM8 is required for virus-induced IFN response in human plasmacytoid dendritic cells

Ghizlane Maarifi[1]*, Nikaïa Smith[2,3]*, Sarah Maillet[1], Olivier Moncorgé[1], Célia Chamontin[1], Joanne Edouard[4], Frédéric Sohm[4], Fabien P. Blanchet[1], Jean-Philippe Herbeuval[2], Georges Lutfalla[5], Jean-Pierre Levraud[6], Nathalie J. Arhel[1], Sébastien Nisole[1†]

Plasmacytoid dendritic cells (pDCs) play a crucial role in antiviral innate immunity through their unique capacity to produce large amounts of type I interferons (IFNs) upon viral detection. Tripartite motif (TRIM) proteins have recently come forth as important modulators of innate signaling, but their involvement in pDCs has not been investigated. Here, we performed a rationally streamlined small interfering RNA (siRNA)–based screen of TRIM proteins in human primary pDCs to identify those that are critical for the IFN response. Among candidate hits, TRIM8 emerged as an essential regulator of IFN regulatory factor 7 (IRF7) function. Mechanistically, TRIM8 protects phosphorylated IRF7 (pIRF7) from proteasomal degradation in an E3 ubiquitin ligase–independent manner by preventing its recognition by the peptidyl-prolyl isomerase Pin1. Our findings uncover a previously unknown regulatory mechanism of type I IFN production in pDCs by which TRIM8 and Pin1 oppositely regulate the stability of pIRF7.

INTRODUCTION

Type I interferons (IFNs) are the main orchestrators of the antiviral innate immune response. Their expression is induced following the recognition of pathogen-associated molecular patterns (PAMPs) by several classes of pattern recognition receptors (PRRs), including Toll-like receptors (TLRs) and RIG-I–like receptors (*1*). Intracellular signaling pathways downstream of PRRs lead to the phosphorylation of IFN regulatory factor 7 (IRF7) and IRF3, thus promoting their dimerization and translocation to the nucleus where they activate the transcription of type I IFN genes.

IRF3 and IRF7 share some structural and functional similarities, but they hold widely distinct roles in the systemic response to infection. While the expression of IRF7 requires the previous activation of IRF3 in most cell types, it is ubiquitously and constitutively expressed in plasmacytoid dendritic cells (pDCs), a rare DC subtype that plays a pivotal role in immunity (*2*, *3*). Constitutive IRF7 expression allows pDCs to rapidly produce large amounts of type I IFN in response to viruses, making them a professional type I IFN–producing cell type that accounts for most circulating type I IFN during an antiviral innate immune response (*2*, *3*).

pDCs are activated following the sensing of viral RNA or DNA by TLR7 and TLR9, respectively. PAMP detection causes the adaptor protein MyD88 to engage a multiprotein signaling complex composed of IRAK1, IRAK4, TRAF6, and IKKα. The recruitment of IRF7 to this complex triggers its phosphorylation, dimerization, and translocation to the nucleus (*4*). These signaling pathways are tightly regulated at multiple levels both by potent activators that implement a rapid and robust IFN response following infection and by equally potent inhibitors that prevent an exacerbated or prolonged activation that may lead to adverse pathogenic effects (*5*, *6*).

Proteins of the tripartite motif (TRIM) family have recently emerged as potentially important regulators of innate immune pathways. TRIM proteins are a large family of E3 ubiquitin ligases that share an N-terminal TRIM composed of a RING domain, one or two B boxes, and a coiled coil domain (*7*, *8*). Among the 75 human TRIM proteins, some have been described as critical immunoregulatory proteins, acting at multiple steps of signaling pathways (*9*–*12*). However, although the implication of a few TRIM proteins has been extensively studied and validated in appropriate primary cells and/or in mouse models, the comparative profiling of all TRIM proteins in the relevant type I IFN–producing cells in vivo has not been performed. We report here the results of the first small interfering RNA (siRNA) screen performed in human primary pDCs, which allowed us to identify TRIM8 as an essential positive regulator of the virus-induced IFN response.

RESULTS

TRIM8, TRIM20, TRIM21, TRIM22, TRIM28, TRIM36, TRIM38, TRIM46, and TRIM49 identified as potential regulators of IFN response in human pDCs

Because human primary pDCs account for less than 0.5% of peripheral blood mononuclear cells (PBMCs), a comprehensive siRNA screen of the entire TRIM protein family cannot be achieved on single blood donors. Therefore, to perform a rationally streamlined screen of TRIM proteins that could conceivably be implicated in TLR downstream signaling cascade in pDC, we first determined which TRIM family members are constitutively expressed in human pDCs. We purified primary human pDCs from the blood of three healthy donors (fig. S1A) and performed a systematic transcriptional profiling of all *TRIM* genes by reverse transcription-quantitative polymerase chain reaction (RT-qPCR) (Table 1). Our results indicated that, among the 75 known *TRIM* genes, only 18 are expressed at detectable levels under steady-state conditions (Fig. 1A). Among them, TRIM8, TRIM22, and TRIM28 had the highest constitutive expression in resting pDCs.

Next, we investigated which *TRIM* genes are induced in pDCs following activation by RNA viruses and could thus be involved in a feedback loop to control the signaling pathway leading to IFN production. Primary pDCs were stimulated with HIV-1 or influenza A virus

[1]IRIM, CNRS, Université de Montpellier, Montpellier, France. [2]CBMIT, CNRS, Université Paris Descartes, Paris, France. [3]Institute of Molecular Virology, Ulm University Medical Center, Ulm, Germany. [4]AMAGEN, CNRS, INRA, Université Paris-Saclay, Gif-sur-Yvette, France. [5]DIMNP, CNRS, Université de Montpellier, Montpellier, France. [6]Unité Macrophages et Développement de l'Immunité, CNRS, Institut Pasteur, Paris, France.
*These authors contributed equally to this work.
†Corresponding author. Email: sebastien.nisole@irim.cnrs.fr

Table 1. List of the 114 transcripts simultaneously quantified by RT-qPCR profiling, including 6 housekeeping genes (1 to 6), 75 TRIM genes (7 to 81), 17 ISGs (82 to 98), 9 IFNs (99 to 107), and 7 inflammatory cytokines or chemokines (108 to 114). For each transcript, the official name, the alias name, if any, and the RefSeq accession number are indicated.

	Transcript	Alias	Ref Seq		Transcript	Alias	Ref Seq		Transcript	Alias	Ref Seq
1	SDHA		NM_004168	39	TRIM35		NM_171982	77	TRIM74		NM_198853
2	TBP		NM_003194	40	TRIM36		NM_018700	78	TRIM75P	TRIM75	NG_016722
3	POLR2A		NM_000937	41	TRIM37		NM_015294	79	CMYA5	TRIM76	NM_153610
4	PPIA	CypA	NM_021130	42	TRIM38		NM_006355	80	TRIM77		NM_001146162
5	PPIB	CypB	NM_000942	43	TRIM39		NM_021253	81	TRIML1		NM_178556
6	B2M		NM_004048	44	TRIM40		NM_138700	82	IFIT1		NM_001548
7	MID2	TRIM1	NM_012216	45	TRIM41		NM_201627	83	IFIT2		NM_001547
8	TRIM2		NM_015271	46	TRIM42		NM_152616	84	IFIT3		NM_001549
9	TRIM3		NM_006458	47	TRIM43		NM_138800	85	IFITM1		NM_003641
10	TRIM4		NM_033017	48	TRIM44		NM_017583	86	IFITM2		NM_006438
11	TRIM5		NM_033093	49	TRIM45		NM_025188	87	IFITM3		NM_021034
12	TRIM6		NM_058166	50	TRIM46		NM_025058	88	ISG15		NM_005101
13	TRIM7		NM_033342	51	TRIM47		NM_033452	89	ISG20		NM_002201
14	TRIM8	GERP	NM_030912	52	TRIM48		NM_024114	90	EIF2AK2	PKR	NM_002759
15	TRIM9		NM_015163	53	TRIM49		NM_020388	91	Mx1		NM_001144925
16	TRIM10		NM_006778	54	TRIM50		NM_178125	92	Mx2		NM_002463
17	TRIM11		NM_145214	55	SPRYD5	TRIM51	NM_032681	93	TNFSF10	TRAIL	NM_001190942
18	TRIM13		NM_005798	56	TRIM52		NM_032765	94	APOBEC3A		NM_145699
19	TRIM14		NM_014788	57	TRIM53AP	TRIM53	NR_028346.1	95	APBEC3G		NM_021822
20	TRIM15		NM_033229	58	TRIM54		NM_187841	96	BST2	Tetherin	NM_004338
21	TRIM16		NM_006470	59	TRIM55		NM_184087	97	RSAD2	Viperin	NM_080657
22	TRIM17		NM_016102	60	TRIM56		NM_030961	98	DDX58	RIG-I	NM_014314
23	MID1	TRIM18	NM_000381	61	TRIM58		NM_015431	99	IFNA1		NM_024013
24	PML	TRIM19	NM_033238	62	TRIM59		NM_173084	100	IFNA2		NM_000605
25	MEFV	TRIM20	NM_000243	63	TRIM60		NM_152620	101	IFNA4		NM_021068
26	TRIM21	Ro52	NM_003141	64	TRIM61		NM_001012414	102	IFNA5		NM_002169
27	TRIM22	Staf50	NM_006074	65	TRIM62		NM_018207	103	IFNA8		NM_002170
28	TRIM23		NM_001656	66	TRIM63		NM_032588	104	IFNB1		NM_002176
29	TRIM24		NM_003852	67	TRIM64		XM_061890	105	IFNL1	IL29	NM_172140
30	TRIM25		NM_005082	68	TRIM65		NM_173847	106	IFNL2	IL28A	NM_172138
31	TRIM26		NM_003449	69	TRIM66		NM_014818	107	IFNG		NM_000619
32	TRIM27		NM_006510	70	TRIM67		NM_001004342	108	IL1B		NM_000576
33	TRIM28		NM_005762	71	TRIM68		NM_018073	109	IL4		NM_000589
34	TRIM29		NM_012101	72	TRIM69		NM_182985	110	IL6		NM_000600
35	TRIM31		NM_007028	73	TRIM16L	TRIM70	NM_001037330	111	IL10		NM_000572
36	TRIM32		NM_012210	74	TRIM71		NM_001039111	112	TNF		NM_000594
37	TRIM33		NM_015906	75	TRIM72		NM_001008274	113	CXCL8	IL8	NM_000584
38	TRIM34		NM_021616	76	TRIM73		NM_198924	114	CXCL10	IP-10	NM_001565

(IAV), which potently activate pDCs through TLR7 within endosomes (*13*, *14*). The triggering of the TLR7/IRF7 signaling pathway was monitored by measuring both intracellular (Fig. 1B) and secreted (Fig. 1, C and D) type I IFNs, which indicated that both viruses achieved comparable levels of activation at the doses of inoculum used. As previously reported, activated pDCs produce large amounts of type I IFNs but no IFN-γ (Fig. 1C) (*3*). We then performed the transcriptional profiling of all 75 *TRIM* genes in HIV- or IAV-activated pDCs purified from the blood of three individual donors. We quantified simultaneously the expression of 114 genes, including 6 housekeeping genes, 17 IFN-induced genes (ISGs), 16 virus-induced cytokines and chemokines, and the 75 human *TRIM* genes (Table 1). As shown in Fig. 1E, while most tested cytokines, chemokines, and ISGs were highly induced by both viruses, less than half of TRIM transcripts were up-regulated by either HIV-1 or IAV, and only a handful were induced by both. Among them, TRIM20, TRIM36, TRIM46, and TRIM49 had the strongest activation profiles, ranging from 6-fold (TRIM49) to 107-fold (TRIM20) increase upon HIV-1 infection and from 9-fold (TRIM46) to 44-fold (TRIM20) increase following IAV detection (Fig. 1E and fig. S1B).

These profiling experiments allowed us to streamline our analysis to seven key TRIM proteins that were either expressed at high constitutive levels (TRIM8, TRIM22, and TRIM28) or induced following viral activation (TRIM20, TRIM36, TRIM46, and TRIM49) in human pDCs. These TRIM proteins identified as the most relevant to pDC biology could constitute potential regulators of IFN production in virus-activated pDCs. On the basis of the abundant literature on TRIM proteins, we added two other candidates to our short list, TRIM21 and TRIM38, which were moderately up-regulated by both viruses, by four- and twofold, respectively (Fig. 1E). Although their function was not investigated in pDCs, their mode of action suggests that they

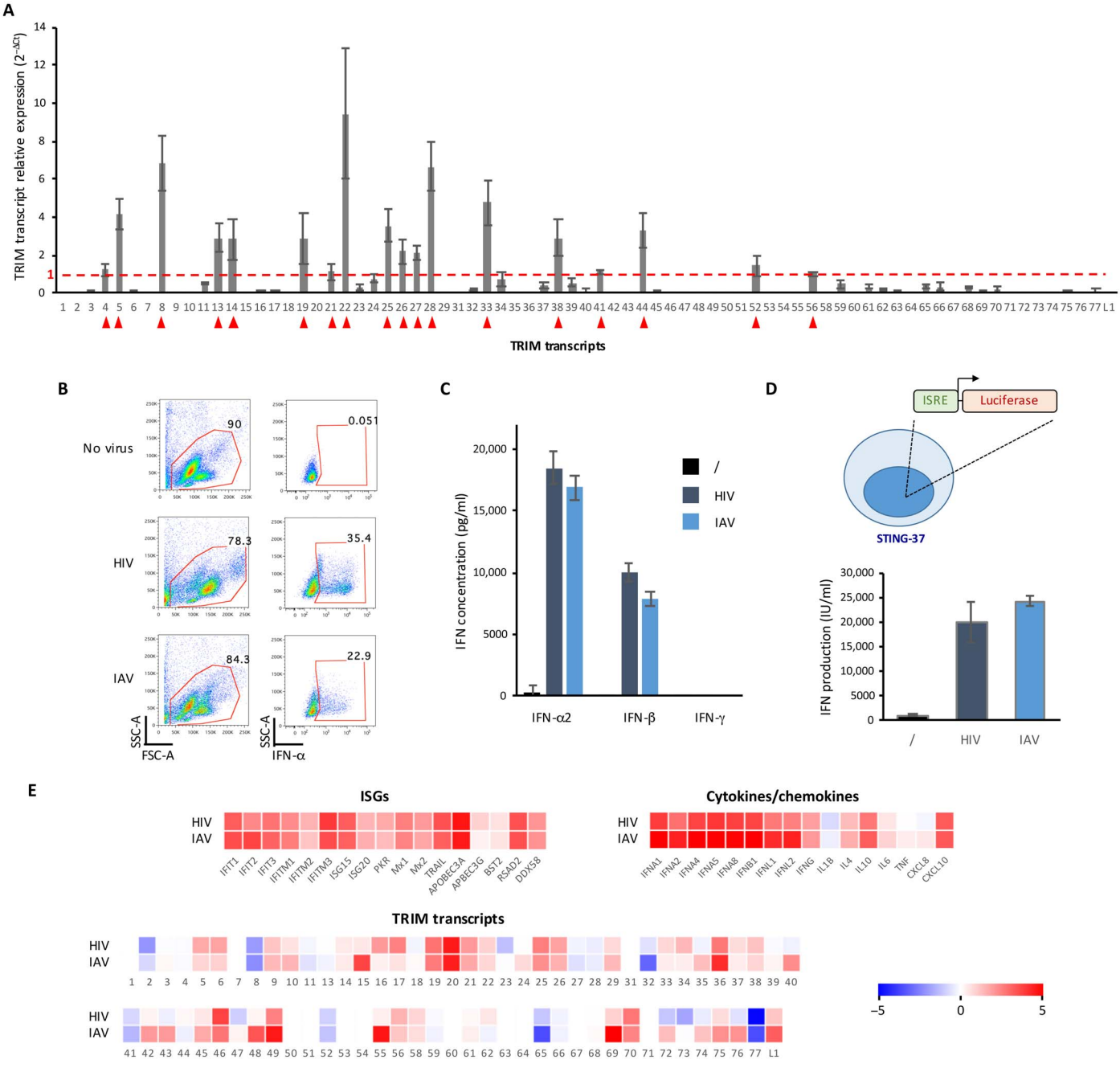

Fig. 1. Constitutively expressed and virus-induced *TRIM* genes in human primary pDCs. (**A**) Systematic analysis of constitutive expression of all human TRIM genes in pDCs by RT-qPCR analysis. Data represent the mean ± SD of independent experiments performed in duplicate on purified pDCs from three different blood donors. Red arrows point to TRIM genes that are constitutively expressed at detectable levels above the geometric mean of the six different housekeeping genes ($2^{-\Delta Ct} > 1$). (**B**) Purified pDCs were stimulated overnight with HIV-1 MN AT-2 or influenza A virus (IAV). Cytokine secretion was blocked for 12 hours using BFA at 1 μg/ml. Intracellular IFN-α was measured by fluorescence-activated cell sorting (FACS) after fixation and saponin permeabilization. (**C** and **D**) IFN secreted in the culture medium by virus-activated pDCs was titrated using two different techniques: The concentration of IFN-α2, IFN-β, and IFN-γ was quantified by the multiplex bead-based immunoassay LEGENDplex (BioLegend) (C), or global (type I and type II) IFN activity was quantified using the STING-37 reporter cell line, which expresses luciferase under the control of five IFN-stimulated response elements (ISRE) (D). (**E**) Purified pDCs from three donors were activated with HIV-1 MN AT-2 or IAV for 16 hours, and the transcriptional profiles of 114 genes [6 housekeeping genes, 17 IFN-induced genes (ISGs), 16 virus-induced cytokines and chemokines, and the 75 human TRIM genes] were analyzed simultaneously by RT-qPCR. The expression of each transcript was normalized to the geometric mean of a set of stably expressed reference genes (*SDHA*, *PPIB*, *TBP*, *POLR2A*, *PPIA*, and *B2M*). Data represent the mean of three independent experiments performed in duplicate on purified pDCs from different blood donors. Values were converted to $\log_2$ and represented as heat maps. Raw data are shown in fig. S1B.

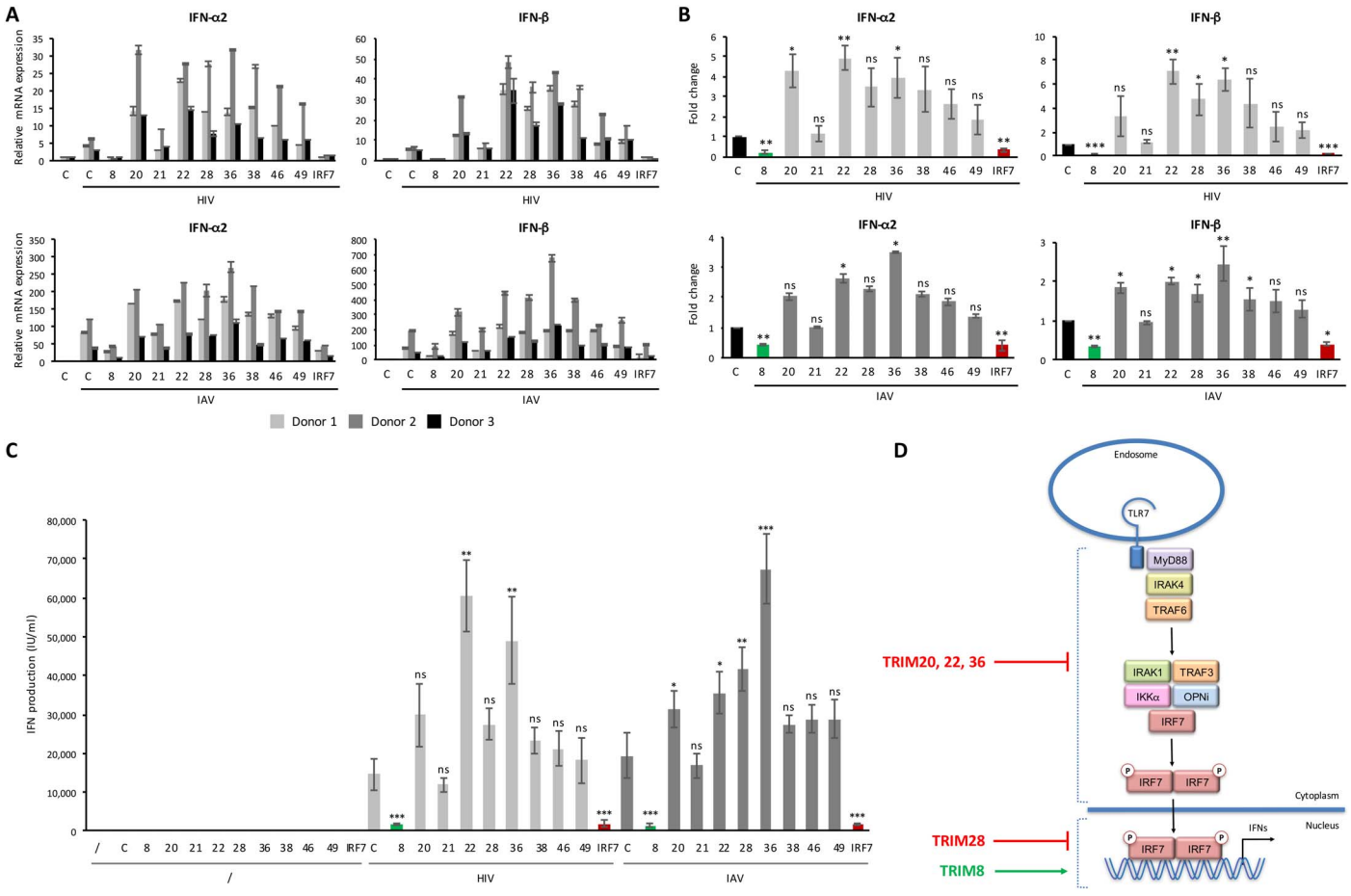

Fig. 2. Effect of TRIM gene silencing on virus-induced IFN response in human primary pDCs. (**A** to **C**) Purified pDCs from three donors were transfected with nontargeting siRNA (C) or with siRNA targeting selected TRIM transcripts (TRIM8, TRIM20, TRIM21, TRIM22, TRIM28, TRIM36, TRIM38, TRIM46, or TRIM49) or IRF7 as a control. After 24 hours, pDCs were activated with HIV-1 MN AT-2 or IAV for 16 hours before the expression of type I IFN was determined both at the transcript level by RT-qPCR (A and B) and at the protein level in the culture medium (C). The relative expression of IFN-α2 and IFN-β transcripts in activated pDCs is represented as mean values ± SD, with each bar representing a single donor (A) and as mean fold change of all donors relative to control siRNA (B). (C) For the quantification of IFN in the culture medium, STING-37 cells were incubated for 24 hours with the supernatant of activated pDCs or with known concentrations of recombinant IFN-α2. Statistical significance (*P* value) was calculated by one-way analysis of variance (ANOVA). **P* < 0.05; ***P* < 0.01; ****P* < 0.001; ns, not significant. (**D**) Schematic model of TRIM proteins identified as positive (in green) and negative (in red) regulators of TLR7-dependent IFN response in human pDCs. The putative compartment (cytoplasm or nucleus) where TRIM proteins act is based on their known subcellular localization (*8*).

could be relevant negative regulators of IFN response. In particular, TRIM21 was described as a negative regulator of IRF7 (*15*), whereas TRIM38 was found to promote TRAF6 degradation (*16*).

TRIM8, TRIM20, TRIM22, TRIM28, and TRIM36 are regulators of IFN response in virus-activated human pDCs

To determine the role of the selected TRIM proteins on innate signaling pathways downstream of TLR7, we performed an siRNA-based screen using a robust method that we published previously (*17*). Purified pDCs from three blood donors were transfected with each TRIM-specific siRNA pool and treated with HIV-1 or IAV to trigger an IFN response. An siRNA directed against IRF7 was used as control, because IRF7 silencing abolishes IFN production in pDCs (*17*). All targeted transcripts were knocked down, with mean efficiencies ranging between 60 and 75% (fig. S1C).

We first evaluated the effect of TRIM knockdown on type I IFN transcription by RT-qPCR. While TRIM21, TRIM46, and TRIM49 knockdowns did not affect the transcription of type I IFN genes, silencing of TRIM20, TRIM22, TRIM28, and TRIM36 led to a significant increase in IFN response in response to both HIV-1 and IAV (Fig. 2, A and B). TRIM8 knockdown virtually abolished IFN-α and IFN-β transcription to the same extent as IRF7 silencing (Fig. 2, A and B). These results were confirmed at the protein level by titrating IFNs in the culture supernatant of virus-activated pDCs (Fig. 2C). Together, our siRNA screen led to the identification of TRIM20, TRIM22, TRIM28, and TRIM36 as negative regulators of IFN response in human pDCs, whereas TRIM8 was the only positive regulator identified. These results are summarized in Fig. 2D.

TRIM8 is a nuclear protein that is required for pIRF7-induced IFN production in pDCs

The fact that TRIM8 knockdown almost completely abolished IFN production was notable and suggested that TRIM8 could act as an essential positive regulator of the antiviral response. To gain understanding of the components of the signaling cascade that TRIM8 might engage with, we first examined its subcellular localization in

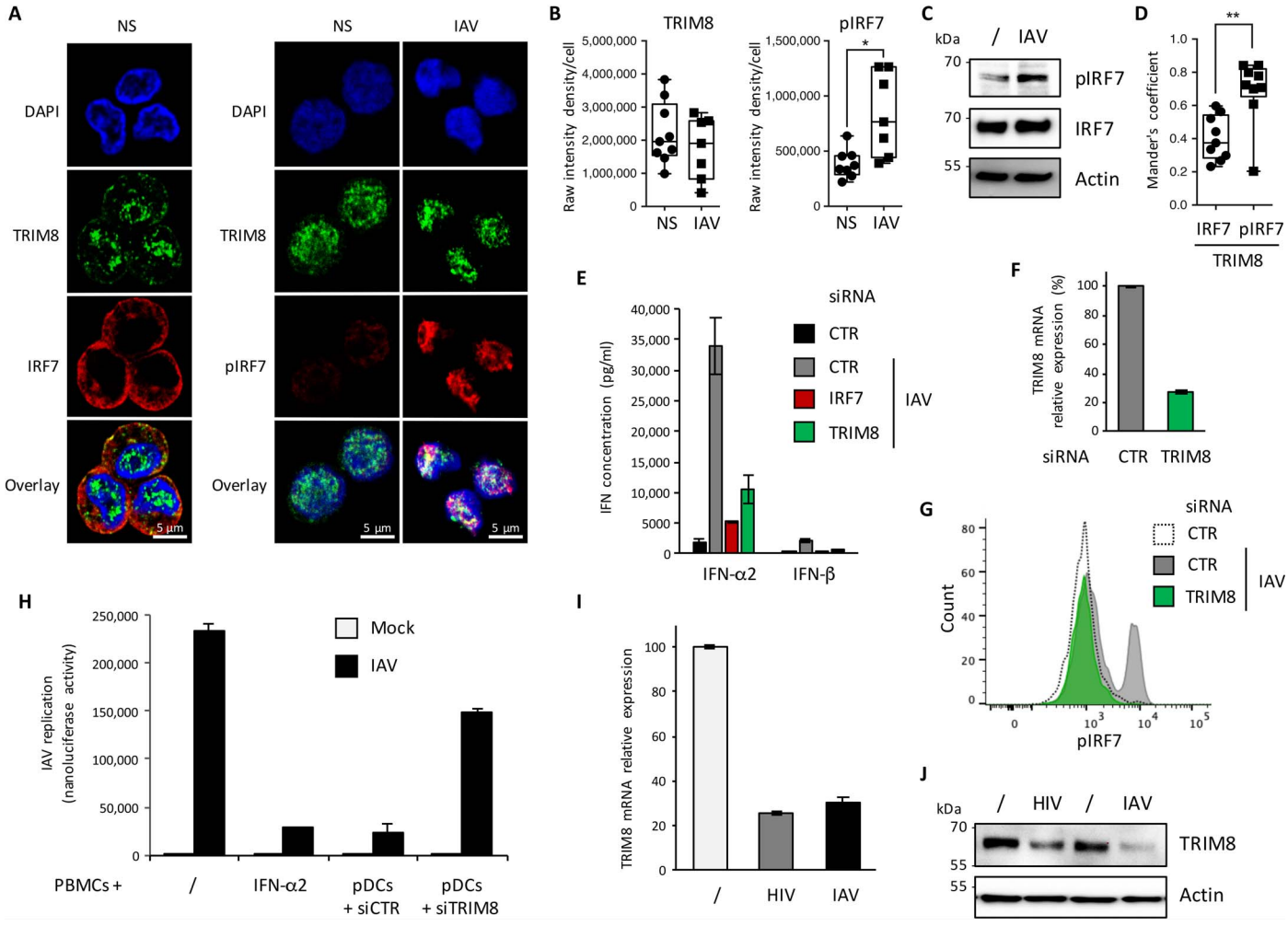

Fig. 3. TRIM8 knockdown inhibits IFN secretion through a decrease of pIRF7 in human primary pDCs. (**A**) Subcellular localization of TRIM8 and IRF7 or pIRF7 was visualized by immunofluorescent confocal microscopy on naive pDCs (NS) or pDCs stimulated for 6 hours with IAV. (**B**) Raw intensity density per cell of TRIM8 and pIRF7 staining was measured using ImageJ software. Data represented by box and whiskers with median ± min to max represent the analysis of 30 cells from nine different fields. *P < 0.05, by Mann-Whitney test. (**C**) Expression of pIRF7 and IRF7 in IAV-stimulated pDCs was assessed by Western blot. (**D**) Mander's coefficients were determined using the ImageJ JACoP plug-in to evaluate the colocalization between IRF7 and TRIM8 or between pIRF7 and TRIM8 in unstimulated or IAV-stimulated cells, respectively. The analysis was performed on 30 cells from nine different fields. **P < 0.01, by Mann-Whitney test. (**E** to **G**) Human pDCs were transfected with nontargeting siRNA (CTR) or with a TRIM8-specific siRNA and activated 24 hours later with IAV for 16 hours. (E) The concentration of IFN-α2 and IFN-β secreted in the culture medium by IAV-activated pDCs was quantified with the multiplex bead-based immunoassay LEGENDplex (BioLegend). (F) TRIM8 expression was verified by RT-qPCR. To quantify the amount of pIRF7 by flow cytometry, cells were fixed, permeabilized, and labeled with mouse Alexa Fluor 488 anti-IRF7 (pS477/pS479) antibody. (G) Representative flow cytometry histogram of pIRF7 expression in nonactivated control (dotted line), IAV-stimulated control (gray), or TRIM8 knockdown pDCs (green). (**H**) pDCs were transfected with nontargeting siRNA (siCTR) or with a TRIM8-specific (siTRIM8) siRNA and activated for 16 hours with R848 (5 µg/ml). Activated pDCs were then cocultured with autologous PBMCs at a ratio of 1:10. After 24 hours of coculture, PBMCs were mock-infected (/) or infected with 2.5 × 10^4 PFU/well of the IAV nanoluciferase-expressing reporter virus for 24 hours before nanoluciferase activity was measured on an Infinite F200 Pro (Tecan) plate reader. As controls, PBMCs were cultivated without pDCs and were either left untreated (/) or treated with 1000 IU of IFN-α2 before challenged with the same dose of IAV reporter virus. Data represent the mean ± SD of one experiment performed in triplicate, representative of two independent experiments performed on cells from two blood donors. (**I** and **J**) Human pDCs were activated with HIV-1 MN or IAV, and TRIM8 expression was determined by RT-qPCR (I) and Western blot (J) 6 or 24 hours after stimulation, respectively.

primary human pDCs. We observed that TRIM8 is predominantly expressed in the nucleus in both resting and IAV-stimulated pDCs, suggesting that viral activation does not induce its relocalization (Fig. 3, A and B). Because the signaling cascade leading to the activation of IRF7 takes place exclusively in the cytoplasm, the nuclear localization of TRIM8 suggested that it might be involved in nuclear steps following the nuclear translocation of phosphorylated IRF7 (pIRF7) dimers and before the nuclear export of type I IFN transcripts (*18*). Stimulation of pDCs with IAV led to IRF7 phosphorylation (Fig. 3C) and translocation into the nucleus (Fig. 3A), where it was found to colocalize with TRIM8 with a Mander's coefficient of 0.7 ± 0.2 (Fig. 3D). Furthermore, while the amount of IFN-α and IFN-β secreted by IAV-activated pDCs was markedly inhibited (Fig. 3, E and F), TRIM8 knockdown also led to a profound decrease of the amount of pIRF7 (Fig. 3G), further suggesting that TRIM8 might stabilize pIRF7 in the nucleus. In the organism, pDCs can protect surrounding cells from viral infections through the secretion of type I IFNs. Because TRIM8 knockdown causes a marked decrease of IFN

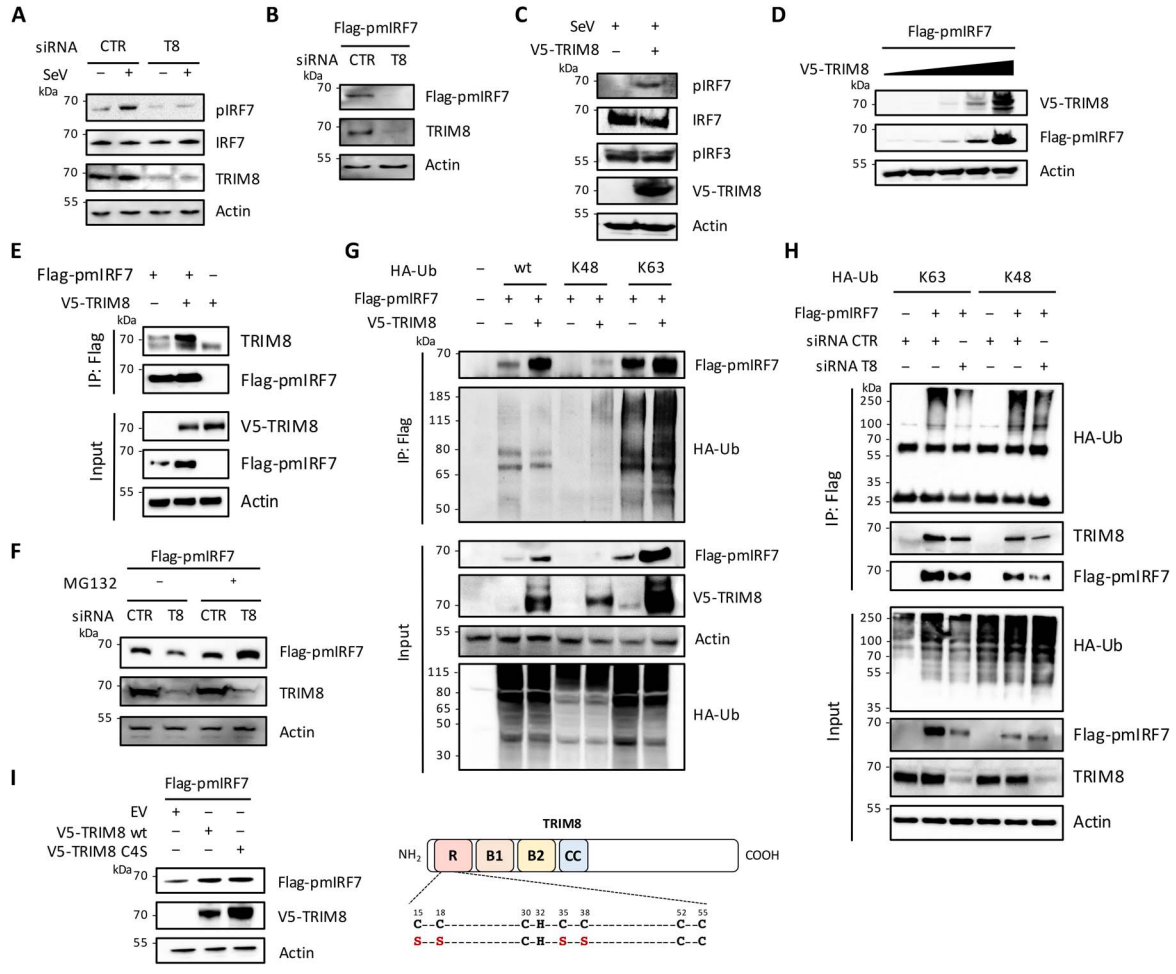

Fig. 4. TRIM8 regulates pIRF7 stability independently of its E3 ubiquitin ligase activity. (**A**) HEK293T cells were transfected with nontargeting control (CTR) or TRIM8-specific (T8) siRNA. Twenty-four hours after transfection, expression of endogenous IRF7 was induced by treating the cells with 1000 IU of IFN-α2 for 16 hours and cells were infected with SeV to trigger IRF7 phosphorylation. Equal amounts of cell extracts were analyzed by Western blot for the expression of TRIM8, IRF7, and pIRF7. (**B**) HEK293T cells expressing Flag-tagged phosphomimetic IRF7 (S477D/S479D) construct (Flag-pmIRF7) were transfected with nontargeting control (CTR) or TRIM8-specific siRNA. After 48 hours, whole-cell lysates were analyzed by Western blot with anti-Flag or anti-TRIM8 antibodies (Abs). (**C**) HEK293T cells were treated with 1000 IU of IFN-α2 for 16 hours and transfected or not with a plasmid expressing V5-TRIM8. The expression of endogenous IRF7, pIRF7, and pIRF3 following SeV infection was evaluated by Western blot. (**D**) Whole-cell lysates obtained from HEK293T cells expressing Flag-pmIRF7 and transfected with increasing amounts of V5-TRIM8 for 48 hours were subjected to Western blot analysis using anti-Flag or anti-V5 antibodies. (**E**) Flag-pmIRF7–expressing HEK293T cells were transfected with V5-TRIM8. After IP using anti-Flag antibodies, TRIM8 was detected using anti-V5 antibodies. **(F)** HEK293T cells expressing Flag-pmIRF7 were transfected with either a nontargeting siRNA (CTR) or an siRNA targeting TRIM8 for 48 hours. Six hours before cell extraction, cells were treated with MG132 to block proteasomal degradation. Expression of Flag-pmIRF7 and TRIM8 was assessed by Western blot using anti-Flag and anti-TRIM8 antibodies, respectively. (**G**) Lysates from HEK293T cells cotransfected with Flag-pmIRF7, V5-TRIM8, and empty vector (EV), HA-Ub (wt), HA-Ub (K48), or HA-Ub (K63) plasmids were subjected to IP with anti-Flag antibody followed by Western blot analysis with anti-Flag, anti-V5, or anti-HA antibodies. (**H**) HEK293T were cotransfected with Flag-pmIRF7 and HA-Ub (K63) or HA-Ub (K48) plasmids and with nontargeting control (CTR) or TRIM8-specific siRNA. After 48 hours, whole-cell lysates were subjected to IP with anti-Flag antibody followed by Western blot analysis with anti-Flag, anti-TRIM8, and anti-HA antibodies. (**I**) Flag-pmIRF7–expressing HEK293T cells were transfected with V5-TRIM8 wt, V5-TRIM8 mutant C15S/C18S/C35S/C38S (V5-TRIM8 C4S), or empty vector. After 48 hours, cell extracts were subjected to Western blot analysis using anti-Flag or anti-V5 antibodies. All panels show typical results representative of at least two independent experiments.

production by activated pDCs, it is also likely to inhibit their antiviral functions. To formally demonstrate this, we showed that pDCs transfected with a nontargeting siRNA and activated with the TLR7 agonist R848 can protect autologous PBMCs from IAV infection, whereas TRIM8-silenced pDCs cannot (Fig. 3H).

While TRIM8 appears essential for IFN response in pDCs, we also found that its expression was down-regulated following viral activation (Fig. 1E). We further confirmed this observation by showing that TRIM8 expression is diminished upon activation of pDCs with either HIV or IAV both at the mRNA (6 hours after stimulation; Fig. 3I) and at the protein level (24 hours after stimulation; Fig. 3J), thus suggesting that TRIM8 expression is regulated by a negative feedback loop.

TRIM8 stabilizes pIRF7 through an E3 ubiquitin ligase–independent mechanism

To obtain mechanistic insight into the regulatory role of TRIM8, we took advantage of a simpler and more versatile cell model, human

embryonic kidney (HEK) 293T cells, in which TRIM8 was also identified as an enhancer of innate immune signaling (*11*). Although IRF7 is not constitutively expressed in HEK293T cells, its expression can be induced to pDC levels by pretreatment with IFN-α (*19*) or by transfection of an expression plasmid. Because HIV-1 and IAV either do not trigger a sufficiently robust IFN response or induce cytotoxicity in this cell type, activation of innate immune pathways was achieved by infection with a defective-interfering Sendai virus (SeV) (Fig. 4A) (*20*). In this model, TRIM8 silencing strongly reduced the amount of pIRF7 following SeV infection (Fig. 4A), confirming the phenotype observed in pDCs upon HIV-1 and IAV treatment. Furthermore, because SeV specifically activates RIG-I (*20*), these results indicate that the effect of TRIM8 on pIRF7 is independent of the upstream pathway that leads to its activation. Next, we evaluated the effect of TRIM8 expression on a phosphomimetic IRF7 mutant (Flag-pIRF7 S477D/S479D), which is constitutively active and can thus stimulate IFN expression in the absence of viral infection (*21*). TRIM8 silencing also led to a lower expression of phosphomimetic IRF7 (Fig. 4B), confirming that TRIM8 is likely to act directly on the activated form of IRF7 that translocates to the nucleus upon PAMP detection. Conversely and as expected, TRIM8 overexpression increased the proportion of phosphorylated form of endogenous IRF7 upon SeV infection (Fig. 4C) as well as the amount of phosphomimetic IRF7 (Fig. 4D). In contrast, TRIM8 overexpression did not increase the amount of pIRF3, thus pointing out the specificity of TRIM8 for pIRF7 (Fig. 4C).

Having confirmed that TRIM8 increases the amount of pIRF7 in both pDCs and HEK293T cells, we addressed how this is achieved. First, we showed that TRIM8 and pIRF7 can be efficiently coimmunoprecipitated (Fig. 4E), indicating that the nuclear colocalization of TRIM8 and pIRF7 (Fig. 3B) corresponds to a physical interaction between the two proteins. Next, we demonstrated that the decrease in pIRF7 expression following TRIM8 knockdown could be reversed by a proteasome inhibitor, indicating that TRIM8 stabilizes pIRF7 by preventing its degradation (Fig. 4F).

Because most regulators of innate immune signaling pathways of the TRIM protein family act through the E3 ubiquitin ligase activity of their RING domain (*10*), we addressed whether the stability of pIRF7 might be regulated by ubiquitination. We therefore tested the propensity of pIRF7 to be ubiquitinated by K48-linked polyubiquitination, which typically targets proteins for proteasomal degradation, or by K63-linked polyubiquitination, which tends to promote stability and activity (*22*, *23*). HEK293T cells overexpressing exogenous pIRF7 were transfected with ubiquitin mutants K48 and K63, which contain arginine substitutions of all lysine residues except at positions 48 and 63, respectively (Fig. 4G). The appearance of ubiquitin chains was assessed specifically on immunoprecipitated pIRF7.

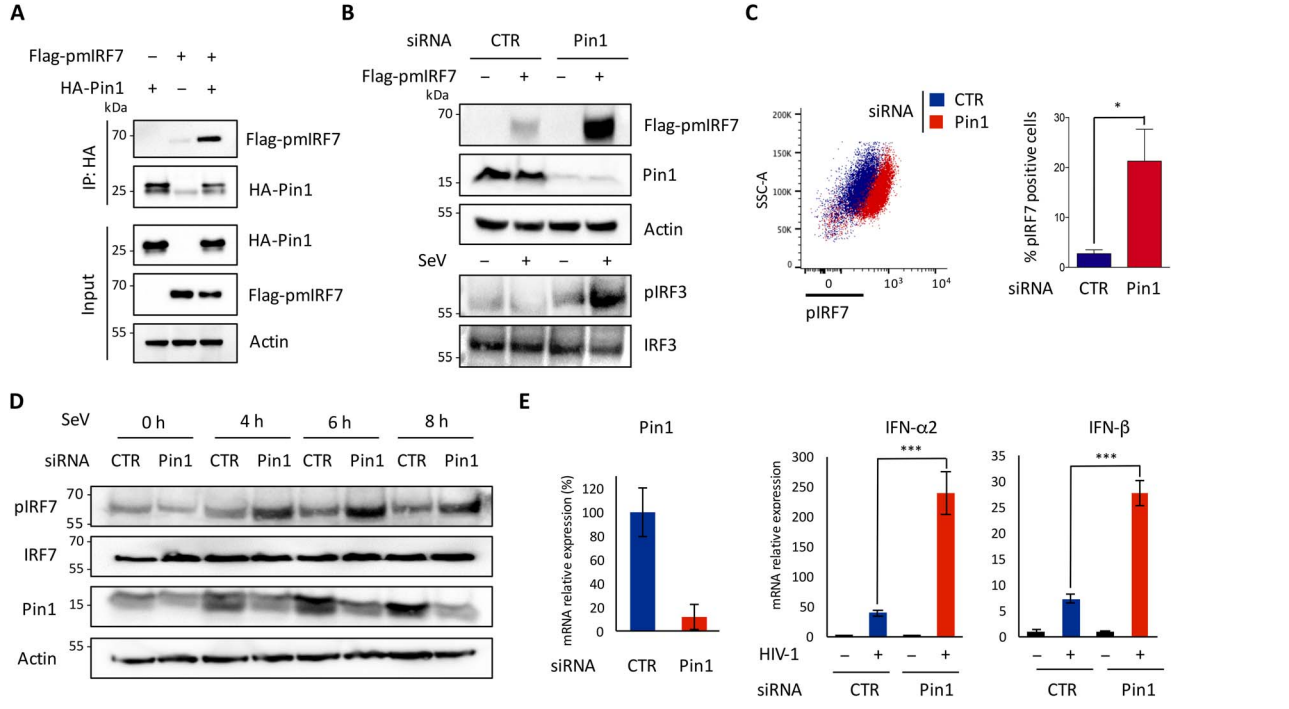

Fig. 5. pIRF7 is a Pin1 substrate. (**A**) HEK293T cells were transfected with HA-Pin1 together with or without Flag-tagged phosphomimetic IRF7 (Flag-pmIRF7). Following IP with anti-HA antibodies, pmIRF7 was revealed using an anti-Flag antibody. (**B**) HEK293T cells were transfected with Flag-pmIRF7 and with nontargeting (CTR) or Pin1-specific siRNA, as indicated. Pin1 and pIRF7 expression was assessed by Western blot using anti-Pin1 or anti-Flag antibodies, respectively. To follow the phosphorylation of endogenous IRF3 as an internal control, cells were also infected with SeV for 6 hours before preparing the extracts, and the expression of IRF3 and pIRF3 was assessed by Western blot. (B) and (C) show typical results representative of at least two independent experiments. (**C**) Pin1 expression was silenced in HEK293T cells using siRNA, while endogenous IRF7 expression was induced by 1000 IU of IFN-α2. Cells were then infected with SeV for 6 hours, and the amount of pIRF7 was evaluated by flow cytometry. Graph shows the mean of three independent experiments ± SD. Statistical significance (*P* value) was determined by Student's *t* test. **P* < 0.05. (**D**) HEK293T cells were transfected with a nontargeting (CTR) or a Pin1-targeting siRNA. IRF7 expression was induced by a 16-hour treatment with 1000 IU of IFN-α2, and activation of IRF7 was triggered by SeV infection. The expression levels of pIRF7, IRF7, and Pin1 were assessed by Western blot at different time points after infection, as indicated. (**E**) Human pDCs from two different donors were transfected with nontargeting siRNA (CTR) or with a Pin1-specific siRNA. Twenty-four hours after transfection, cells were stimulated with HIV-1 for 16 hours, and IFN-α2 and IFN-β mRNA was quantified by RT-qPCR. The results shown are mean ± SD. Statistical significance (*P* value) was determined by Student's *t* test. ****P* < 0.001. Data are representative of three independent experiments.

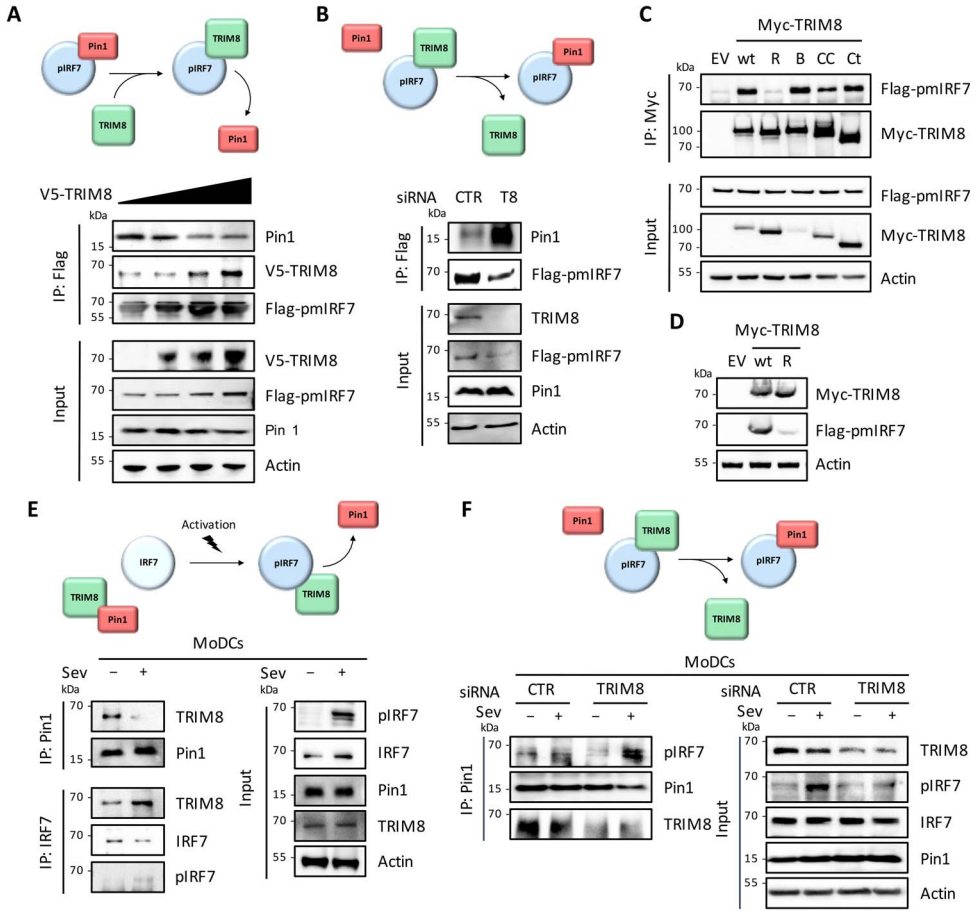

Fig. 6. TRIM8 interferes with the recognition of pIRF7 by Pin1. (**A**) HEK293T cells expressing Flag-tagged phosphomimetic IRF7 (Flag-pmIRF7) were transfected with increasing quantity of the V5-TRIM8 plasmid. Following IP with anti-Flag antibodies, the presence of Pin1, V5-TRIM8, and Flag-pmIRF7 was assessed by Western blot. (**B**) Flag-pmIRF7–expressing HEK293T cells were transfected with a nontargeting (CTR) or a TRIM8-specific siRNA. Flag-pmIRF7 was pulled down using anti-Flag antibodies, and Pin1 was detected by Western blot. (**C**) Flag-pmIRF7–expressing HEK293T cells were transfected with empty vector, Myc-tagged full-length TRIM8 (wt), or TRIM8 deleted from one domain [RING (R), B box (B), coiled coil (CC), or C-terminal domain (Ct)] in the presence of MG132 to prevent pmIRF7 degradation. Following pull-down with anti-Myc antibodies, the presence of pmIRF7 was revealed by Western blot using anti-Flag antibodies. (**D**) HEK293T cells expressing Flag-pmIRF7 were transfected with wt or ΔRING (R) Myc-tagged TRIM8. TRIM8 and pmIRF7 expression was assessed by Western blot using anti-Myc or anti-Flag antibodies, respectively. (**E**) Primary human monocyte-derived dendritic cells (MoDCs) were treated for 16 hours with 1000 IU of IFN-α2 to induce endogenous IRF7 expression and infected or not with SeV for 3 hours to induce its phosphorylation. Following IP with anti-Pin1 or anti-IRF7 antibodies, the presence of pIRF7, IRF7, Pin1, and TRIM8 was assessed by Western blot, as indicated. (**F**) Primary MoDCs were transfected with a nontargeting (CTR) or a TRIM8-specific siRNA, treated for 16 hours with 1000 IU of IFN-α2, and infected or not with SeV for 3 hours. Forty-eight hours after transfection, expression levels of TRIM8, pIRF7, IRF7, and Pin1 were assessed by Western blot. Following IP with anti-Pin1 antibodies, the presence of Pin1, pIRF7, and TRIM8 was assessed by Western blot.

Results suggested that pIRF7 can undergo both K48 and K63 polyubiquitination, leading to its degradation and stabilization, respectively. Overexpressing TRIM8 led to a markedly increased amount of pIRF7 in all conditions (Fig. 4G, Input), as anticipated, and as a consequence, the amount of K48- and K63-linked ubiquitin upon pIRF7 immunoprecipitation (IP) was higher (Fig. 4G, IP: Flag). This suggested that TRIM8 stabilizes pIRF7 independently of its ubiquitination status. Likewise, TRIM8 knockdown triggered pIRF7 degradation in K63-Ub–overexpressing cells (Fig. 4H, Input), and this led to an apparent decreased level of K63-linked ubiquitination of pIRF7 (Fig. 4H, IP: Flag). In cells expressing K48-Ub, which favors pIRF7 degradation, the lower expression of pIRF7 was not further reduced upon TRIM8 knockdown, and no obvious difference in ubiquitination level was observed. Together, these results suggested that pIRF7 polyubiquitination is unlikely to be mediated by TRIM8.

The E3 ubiquitin ligase activity of TRIM proteins is conferred by their RING domain. Therefore, to further demonstrate that the presumed E3 ubiquitin ligase activity of TRIM8 is not implicated in the stabilization of pIRF7, we tested a mutant of TRIM8 in which four of seven cysteine residues that constitute the RING finger domain have been mutated (TRIM8 C4S mutant). As anticipated from the above ubiquitination experiments, the TRIM8 C4S mutant was still able to stabilize pIRF7, thus indicating that TRIM8 acts through an E3 ubiquitin ligase–independent mechanism (Fig. 4I).

TRIM8 prevents Pin1-induced degradation of pIRF7

Although it is unusual to identify a TRIM protein that regulates innate immune signaling independently of its E3 ubiquitin ligase activity, alternative mechanisms have been reported for TRIM21 (*24*) and TRIM19 (*25*), which enhance type I IFN expression by preventing

the recognition of pIRF3 by Pin1 (*26*). Pin1 is a peptidyl-prolyl cis/trans isomerase that specifically recognizes phosphorylated Ser/Thr-Pro motifs and catalyzes the isomerization of the peptide bond, thus affecting the fate of phosphoproteins and, in consequence, the amplitude and duration of biological responses (*27*).

Because IRF7 has not been described as a Pin1 substrate, we focused on determining whether Pin1 can bind to pIRF7 in cells and how this interaction affects pIRF7 function. First, we found that pIRF7 coimmunoprecipitated with Pin1 when both proteins were overexpressed in HEK293T cells, suggesting that pIRF7 could be a Pin1 substrate (Fig. 5A). This was further confirmed by functional experiments, because the knockdown of Pin1 led to a marked accumulation of pIRF7 in cells transfected with the phosphomimetic mutant (Fig. 5B) and increased the amount of endogenously IFN-induced pIRF7 following SeV infection (Fig. 5, C and D). Last, we showed that Pin1 silencing also potentiated the expression of IFN-α and IFN-β transcripts in HIV-stimulated primary pDCs (Fig. 5E). Together, these results suggested that Pin1 can promote a shutdown of IFN expression by inducing pIRF7 degradation, as previously described for pIRF3 (*26*).

Having established that pIRF7 is a Pin1 substrate, we tested whether TRIM8 might stabilize pIRF7 by preventing its Pin1-induced degradation. Because we showed that both TRIM8 (Fig. 4E) and Pin1 (Fig. 5A) can bind to pIRF7, we first asked whether these can attach simultaneously or rather compete with each other for binding to pIRF7. We performed competition experiments between TRIM8 and Pin1 to bind pIRF7 by transfecting increasing amounts of TRIM8 in Pin1- and pIRF7-expressing HEK293T cells. Increasing TRIM8 predictably intensified the pIRF7 band but diminished the amount of Pin1 that was coimmunoprecipitated with pIRF7 (Fig. 6A), while silencing of TRIM8 allowed a better interaction between Pin1 and pIRF7 (Fig. 6B), which combined indicated that TRIM8 interferes with the ability of Pin1 to associate with pIRF7.

To determine which domain of TRIM8 was implicated, we tested a series of TRIM8 deletion mutants for the ability to pull down pIRF7. All mutants maintained the capacity to bind pIRF7 and Pin1 with the notable exception of the TRIM8 ΔRING mutant, indicating that the RING domain was implicated in its interaction with pIRF7 (Fig. 6C). Accordingly, the ΔRING mutant lost the ability to stabilize pIRF7 in cotransfection experiments, confirming that the propensity of TRIM8 to bind pIRF7 is responsible for its ability to stabilize it (Fig. 6D).

Last, to confirm the mechanism of action of TRIM8 in more physiologically relevant cells, we investigated the fate of pIRF7 in primary monocyte-derived DCs (MoDCs) upon SeV infection. We show that, whereas Pin1 and TRIM8 interact in inactivated cells, this interaction is lost upon viral-induced phosphorylation of IRF7 in favor of a pIRF7-TRIM8 interaction (Fig. 6E). Furthermore, as already shown in HEK293T cells, we confirm in MoDCs that TRIM8 knockdown diminished the amount of pIRF7 but favored its interaction with Pin1 (Fig. 6F). These observations performed on endogenous proteins in primary cells further confirm that TRIM8 protects pIRF7 from Pin1 recognition and subsequent degradation.

TRIM8 knockdown diminishes the IFN response in a zebrafish model of chikungunya virus infection

To confirm the role of TRIM8 in an in vivo context, we turned to zebrafish using the chikungunya virus (CHIKV) infection model, which has been shown to induce a strong type I IFN response (*28*). In the absence of a functional adaptive immune system during the first week of embryonic development, the immune protection of zebrafish larva exclusively relies on innate immunity, which makes them a model of choice to study antiviral innate immunity. Furthermore, zebrafish have orthologs of both IRF7 and Pin1 (*29*, *30*). To facilitate the quantification of IFN responses in this model host, we generated a new transgenic reporter zebrafish line, with a membrane-targeted mCherry under the control of the zebrafish *MXA* promoter.

The zebrafish genome contains two TRIM8 co-orthologs named *trim8a* and *trim8b* (*31*). To assess them functionally, we designed antisense morpholinos (MOs) targeting essential splice sites. Injection of either of these MOs to one-cell stage had no visible impact on larval development, yet efficient knockdown was achieved for both genes (fig. S2).

We injected Tg(*MXA*:mCherry) reporter larvae with either trim8-specific MOs and infected them with CHIKV-GFP (green fluorescent protein) at 3 dpf (days postfertilization). Imaging larvae after 48 hours revealed the expected strong induction of the *MXA* reporter, particularly in the liver and gut, consistent with previous ISG expression patterns (Fig. 7A) (*28*). While *trim8a*-depleted larvae showed a response of the same magnitude as controls, the reporter induction was reduced by half in trim8b-depleted larvae (Fig. 7, A and B). Because the IFN response is required for zebrafish larvae to resist CHIKV infection (*32*), we measured disease scores at 72 hours after infection. We observed that *trim8b* morphants, but not *trim8a* morphants, were significantly sicker than controls (Fig. 7C).

Viral burden, as measured by qPCR or GFP fluorescence, tended to be higher in *trim8b* morphants, but this did not reach statistical significance. We reasoned that this could be due to a compensatory effect, as zebrafish larvae express two type I IFN genes in response to CHIKV, *ifnphi1* and *ifnphi3* (*28*). We found that *trim8b* knockdown preferentially affected *ifnphi1* mRNA levels compared to *ifnphi3* (Fig. 7D), thus suggesting that *ifnphi3*-null zebrafish mutants would provide a more appropriate background to test the impact of *trim8b* knockdown on viral infection. We therefore injected control or *trim8b* MOs in homozygous *ifnphi3*-null zebrafish mutant and infected them with CHIKV-GFP. While *ifnphi3*$^{-/-}$ fish injected with a control MO still resisted the infection, the trim8b-depleted ones had a significantly higher disease score (Fig. 7E), reminiscent of IFNR-deficient larvae (*32*), and a significantly higher viral burden, as measured by GFP fluorescence (Fig. 7, F and G) or RT-qPCR (Fig. 7H). These results indicate that in vivo, in the developing zebrafish, TRIM8B positively regulates type I IFN responses and contributes to resistance to viral infection.

DISCUSSION

Over the past decade, an abundant literature described the involvement of various TRIM proteins as positive or negative regulators of innate signaling pathways, leading to the expression of IFNs and inflammatory cytokines (*9*, *10*, *12*). Very few studies, however, evaluated their implication in relevant human primary innate immune cells (*11*).

To evaluate whether some TRIM proteins are key regulators of the IFN response in vivo, we decided to investigate the consequences of their knockdown on the most relevant cell type, namely, pDCs, which are professional type I IFN producer cells.

We conducted a systematic transcriptional profiling of 75 *TRIM* genes in human primary pDCs in steady-state conditions and upon viral activation, and performed an siRNA screen on relevant candidates. The expression profiles that we obtained revealed that only

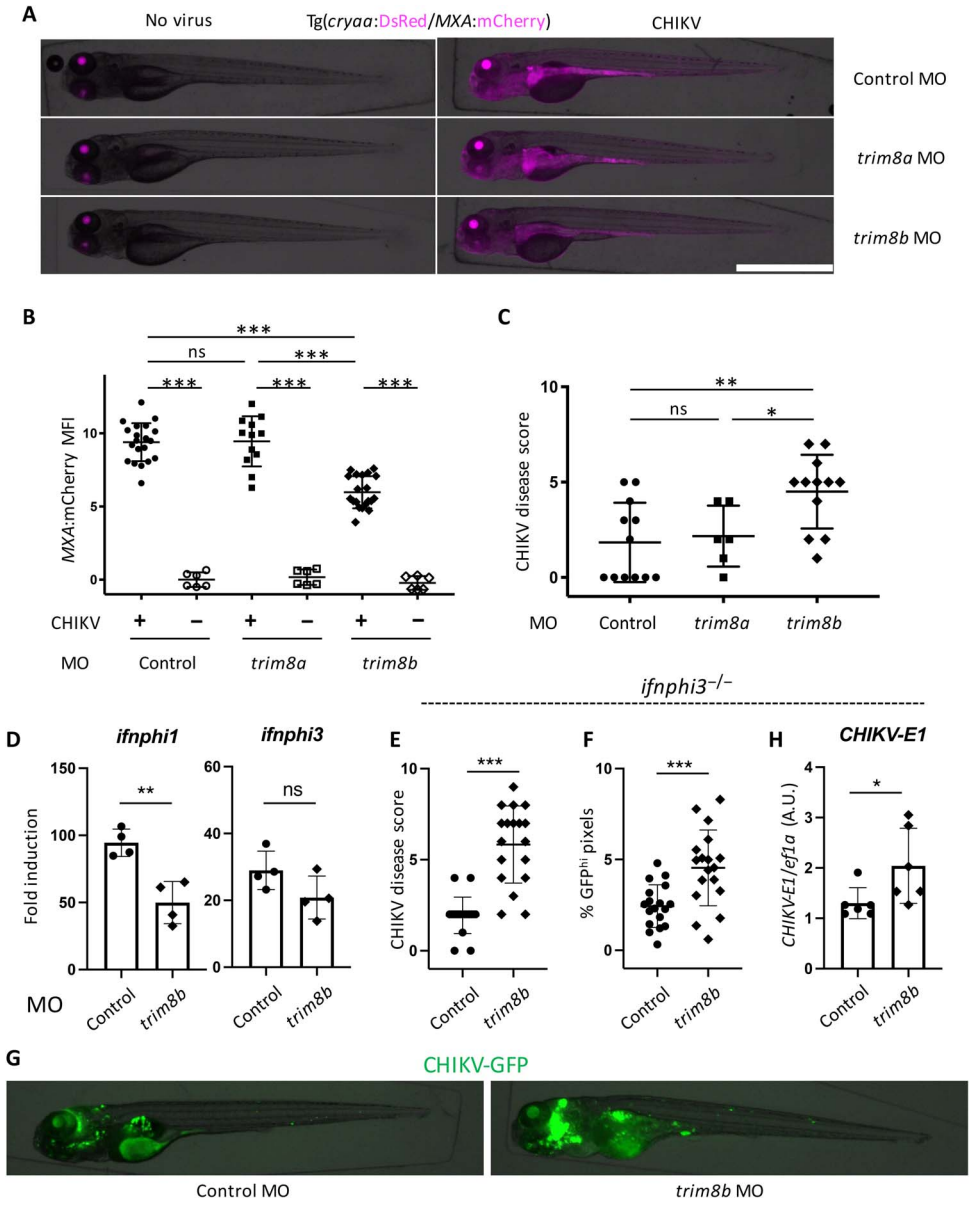

Fig. 7. *trim8b* positively regulates type I IFN responses in zebrafish. (**A**) *MXA* reporter zebrafish embryos were injected at the one-cell stage with control, *trim8a*-targeting, or *trim8b*-targeting morpholinos (MOs) and, at 3 dpf, inoculated or not with CHIKV. After 48 hours, larvae were imaged with a fluorescence microscope. Images are of the lateral view, dorsal to top, anterior to left, and merge of transmitted light image (gray) with red fluorescence (magenta). The red signal in the lens is due to the secondary *cryaa*:DsRed reporter to identify transgene carriers. Scale bar, 1 mm. (**B**) Corresponding quantification of MXA reporter signal. Mean red fluorescence intensity (MFI) was measured posterior to the eyes; average background fluorescence from control larvae was subtracted before plotting the data. (**C**) Disease score assessed 3 days after CHIKV inoculation. (**D**) RT-qPCR measurement of type I IFN gene expression in MO-injected, CHIKV-infected wt larvae 40 hours after infection, displayed as fold induction over uninfected control larvae. (**E** to **H**) Outcome of CHIKV-GFP infection in MO-injected *ifnphi3*$^{ip7/ip7}$ larvae: (E) disease score 3 days after infection; (F) infection level 3 days after infection, quantified by GFP fluorescence, with two representative images shown in (G) as a merge of transmitted light and green fluorescence; (H) RT-qPCR assessment of *CHIKV-E1* transcripts 40 hours after infection. Means ± SD are provided over individual data points. A.U., arbitrary units. (B and C) ANOVA with Sidak's multiple comparisons test was performed. (D to F and J) Unpaired *t* tests were performed. *$P < 0.05$; **$P < 0.01$; ***$P < 0.001$.

a small fraction of *TRIM* genes are expressed in resting pDCs. Similarly, although a large proportion of *TRIM* genes were reported to be induced by IFNs in immune cells (*33*, *34*), here we found that only a limited number of them were actually turned on by RNA viruses in primary pDCs. Hence, the profiling of TRIM expression patterns in pDCs allowed us to better appreciate which family members might be implicated in the IFN response in vivo. In particular, we identified five TRIM proteins that potently regulated IFN response in pDCs by either suppressing signaling downstream of TLR7 (TRIM20, 22, 28, and 36) or promoting IFN production (TRIM8).

Some hits that were obtained here corroborate previous results obtained in cell lines. For instance, TRIM28 was previously found to inhibit IRF7 by promoting its SUMOylation in HEK293T cells (*35*). However, neither TRIM38, which was found to promote TRAF6 degradation in murine macrophages (*16*), nor TRIM21, which was involved in the inhibition of IRF7-driven IFN-α induction in HEK293T

(*15*), was identified as negative regulators of IFN expression in our pDC screen. Conversely, none of the four TRIM proteins that we identified as potent negative regulators in pDCs (TRIM20, 22, 28, and 36) were found to regulate innate immune response when overexpressed in HEK293T cells (*11*). The different cell types or stimulations that were used might explain the discordant phenotypes, and experiments in human pDCs may more closely reflect the IFN response in vivo.

TRIM8 was the only TRIM protein that we found to act as a positive regulator of innate immune signaling in human pDCs. IFN response in TRIM8-silenced cells was reduced at comparable levels to IRF7 knockdown cells, thus suggesting that TRIM8 is not only a positive regulator but also an essential cofactor of IRF7. Thus, our results identified TRIM8 as the first TRIM protein whose expression is crucial for pDCs to mount an efficient antiviral innate response. Despite the recent profusion of research on TRIM proteins, the only other example of a TRIM family member playing an essential role on an innate immune pathway is TRIM25, a key regulator of RIG-I signaling (*36*).

TRIM8, also known as GERP, for glioblastoma-expressed RING finger protein (*37*), is a highly conserved protein implicated in many biological processes, including carcinogenesis and inflammation (*38*–*41*). In particular, TRIM8 was found to regulate various signaling pathways through direct interaction with key effectors including SOCS-1 (*42*), PIAS3 (*43*), or TAK1 (*41*). TRIM8 knockout mice were recently shown to exhibit exacerbated innate immune and inflammatory responses following TLR3 or TLR4 activation, thus suggesting that TRIM8 could also play a negative role on TLR3/4 downstream signaling pathways (*44*).

Using a zebrafish model of CHIKV infection, we showed here that the human TRIM8 ortholog TRIM8B is also an important mediator of IFN response in a teleost fish. Our in vivo loss-of-function approach corroborates previous findings based on in vitro overexpression assays in another fish species (*45*). This role of TRIM8 is thus evolutionary ancient, highlighting its significance. Although IRF7 has a unique ortholog in fish, the existence of pDCs in adult fish is still uncertain (*29*). They are known to be absent in larvae, where their key IFN-expressing role is taken up by neutrophils (*32*). *ifnphi1*-expressing zebrafish larval neutrophils express *irf7* at a high level, whereas ifnphi3 is preferentially induced in nonhematopoietic cells (*32*). The fact that the impact of *trim8b* knockdown is stronger on *ifnphi1* than on *ifnphi3* induction is consistent with an *irf7*-dependent function of TRIM8B, although further work will be required to formally determine whether TRIM8 expression and activity is restricted to specific IFN-expressing cell types in fish.

In primary human pDCs, we showed that TRIM8 knockdown inhibits virus-induced type I IFN gene expression by reducing the amount of the activated form of IRF7, pIRF7. Because TRIM8 is almost exclusively nuclear, we therefore hypothesized that it may act directly on pIRF7 in the nucleus. We confirmed that TRIM8 colocalizes with pIRF7 in the nucleus of activated pDCs, and further showed that TRIM8 binds to pIRF7 and protects it from proteasomal degradation in HEK293T cells. Surprisingly, although most of the TRIM proteins act through their capacity to promote K48- or K63-linked polyubiquitination of proteins (*46*), we determined that pIRF7 stabilization by TRIM8 was independent of its putative E3 ubiquitin ligase activity. Our results show that TRIM8 rather protects pIRF7 from degradation by preventing its recognition by Pin1.

Pin1 specifically recognizes phosphorylated Ser/Thr-Pro motifs and catalyzes the isomerization of the peptide bond, thus affecting the function and/or the stability of target proteins (*27*). Pin1 was identified as a "molecular switch" that modulates the fate of phosphoproteins and therefore the amplitude and duration of a biological response (*27*). Although many cellular substrates have been reported for Pin1, particularly oncogenes and tumor suppressor proteins involved in cell cycle regulation, this is a demonstration that pIRF7 is also a Pin1 substrate.

Some interesting parallels with pIRF3 may be derived from our understanding of pIRF7 regulation and are consistent with the high structural homology shared by the two IRF proteins. Our results showed that Pin1 regulates the stability of pIRF7 by promoting its degradation by the proteasome. Similarly, Pin1 also targets pIRF3 (*26*) and is thought to bring about changes in its conformation that induce its ubiquitination and subsequent degradation by the proteasome (*26*). Furthermore, our data revealed that the negative regulation of pIRF7 by Pin1 is kept in check by TRIM8, which competes with Pin1 for binding to pIRF7, hence promoting the stability and activity of pIRF7, as shown in HEK293T as well as in primary MoDCs. Likewise, TRIM19 (promyelocytic leukemia protein, or PML) and TRIM21 were both shown to prevent pIRF3 recognition by Pin1, thus preventing its degradation (*24*, *25*). TRIM19 sequesters Pin1 within PML nuclear bodies (*25*), whereas the mode of action of TRIM21 may involve preventing the interaction between Pin1 and pIRF3 (*24*) or promoting the K48 polyubiquitination of pIRF3 (*47*, *48*). Although Pin1 can bind both pIRF3 and pIRF7, the effect of TRIM8 is IRF7 specific and does not promote the stabilization of pIRF3.

As the master regulator of type I IFN response, IRF7 expression and activation are tightly regulated by diverse mechanisms acting on multiple steps of the signaling cascade (*18*). First, IRF7 is not constitutively expressed in most cell types but only induced upon viral infections. Second, unlike its closest relative IRF3, IRF7 has a very short half-life (*49*). The only cells that constitutively express high levels of IRF7 are pDCs, but they are very rare and also have a short half-life (*50*). Last, IRF7 is subjected to multiple layers of regulation, including transcriptional, translational, and posttranslational (*18*). In particular, phosphorylation, ubiquitination, SUMOylation, and acetylation of IRF7 have been described as possible controls of its activity and stability (*18*). However, no mechanism had been identified to regulate the stability of the active form of IRF7, pIRF7, to either promote or shut down its activity. Our work identified Pin1 as a terminator of pIRF7-driven type I IFN production and TRIM8 as a Pin1 competitor that protects pIRF7 from Pin1-induced degradation, thus introducing a new mode of regulation to IRF7-dependent IFN production. While TRIM8 emerged as a necessary mediator of virus-induced IFN response in pDCs, our results show that its expression is eventually down-regulated following viral activation, thus suggesting that TRIM8 is regulated by a negative feedback loop. The complexity of the molecular mechanisms developed by cells to regulate IFN expression highlights the fact that a tight control of IFN production is crucial for the organism (*6*). Given the key role of IRF7 in IFN response and the unique potency of pDCs to secrete large amounts of IFNs in response to viral infections, it is not surprising to find particularly effective and complex regulation mechanisms in these cells.

MATERIALS AND METHODS

Plasmids

pRK5 plasmids encoding hemagglutinin (HA)–tagged ubiquitin wild-type (wt), K48, and K63 were provided by T. Dawson (Addgene plasmids #17605, #17606, and #17608) (*51*). Flag-tagged IRF7 wt was purchased from GenScript, and the phosphomimetic Flag-IRF7

(S477D/S479D) was from John Hiscott Pasteur Laboratories (Istituto Pasteur Fondazione Cenci Bolognetti, Rome, Italy) (*21*). HA-Pin1–expressing plasmid was provided by H.-Y. Kao (Research Institute of University Hospitals of Cleveland, Cleveland, OH). Human full-length TRIM8 complementary DNA (cDNA) was isolated from human cDNA library using standard PCR techniques and was subsequently cloned into pcDNA3.1D/V5-His-TOPO plasmid (Invitrogen). The TRIM8 RING mutant C15S-C18S-C35S-C38S was generated by site-directed mutagenesis using the GeneArt Site-Directed Mutagenesis System (Thermo Fisher Scientific). Myc-GFP–tagged TRIM8 deletion mutants were provided by G. Meroni (Department of Life Sciences, University of Trieste, Trieste, Italy).

Viruses

Inactivated AT-2 HIV-1 MN was provided by J. D. Lifson (SAIC-NCI, Frederick, MD) (*52*) and was used at p24 CA equivalent (60 ng/ml) to activate 5×10^4 human pDCs. Infectious human influenza A/Victoria/3/75 (H3N2) virus was used at 1 plaque-forming unit (PFU)/cell to activate pDCs. For IAV infection of human PBMCs (Fig. 3G), we used the IAV Victoria-NanoLuc reporter virus, which has been previously described (*53*). Briefly, the porcine teschovirus P2A sequence and the NanoLuc luciferase gene were introduced in the A/Victoria/3/75 polymerase acidic protein gene. IAV challenges of PBMCs were performed using 2.5×10^4 PFU/well of virus (corresponding to a multiplicity of infection of 0.28). Defective-interfering H4 SeV was provided by D. Garcin (Department of Microbiology and Molecular Medicine, University of Geneva, Geneva, Switzerland) and used at 50 hemagglutination units (HAU)/ml (*20*).

Antibodies

Primary antibodies used in Western blot and IP experiments were rat anti-HA clone 3F10 (Sigma-Aldrich), mouse anti-Flag clone M2 (Sigma-Aldrich), mouse anti-V5 Tag (Thermo Fisher Scientific), mouse anti-TRIM8 (Santa Cruz Biotechnology, sc-398878), mouse anti-IRF7 clone G-8 (Santa Cruz Biotechnology, sc-74472), rabbit anti-pIRF7 (Ser^{477}) clone D7E1W (no. 12390, Cell Signaling), rabbit anti-ubiquitin (linkage-specific K63) clone EPR8590-448 (Abcam), rabbit anti-Pin1 (no. 3722, Cell Signaling), and mouse anti–β-actin (Sigma-Aldrich). Secondary antibodies used were anti-mouse, anti-rat, and anti-rabbit horseradish peroxidase (HRP)–conjugated (GE Healthcare Life Sciences).

For immunofluorescence and flow cytometry, we used Alexa Fluor 488 mouse anti-IRF7 (pS477/pS479) clone K47-671 (BD Biosciences), mouse anti–IFN-α phycoerythrin (PE) clone LT27:295 (Miltenyi Biotec), mouse allophycocyanin (APC) anti–BDCA-4 clone REA380 (Miltenyi Biotec), mouse fluorescein isothiocyanate (FITC) anti-CD123 clone AC145 (Miltenyi Biotec), and rabbit anti-TRIM8 (Thermo Fisher Scientific) antibodies. Secondary antibody (for TRIM8 labeling) was Alexa Fluor 546 goat anti-rabbit (Thermo Fisher Scientific).

Immunoprecipitations

Cells were lysed in IP lysis buffer containing 50 mM tris-HCl (pH 7.4), 150 mM NaCl, 1 mM EDTA, 1% Triton X-100, EDTA-free protease inhibitor cocktail (Roche), and 1 mM phenylmethylsulfonyl fluoride. Cell lysates were incubated overnight at 4°C with anti-Flag M2, anti-HA, or anti–c-Myc agarose affinity gel antibody (Sigma-Aldrich) or anti-IRF7 or anti-Pin1 antibodies and protein G Sepharose beads (Thermo Fisher Scientific). Beads were washed three times and eluted with 2× SDS loading buffer. For immunoblotting, proteins were resolved by SDS–polyacrylamide gel electrophoresis and transferred onto a nitrocellulose membrane.

Blood samples, isolation, and culture of human primary cells

Blood from healthy HIV-1–seronegative blood donors was obtained from "Etablissement Français du sang" (EFS Pyrénées-Méditerranée, convention #21PLER2016-0083, and EFS Cabanel, convention #07/CABANEL/106). PBMCs were isolated by density centrifugation with Lymphoprep medium (STEMCELL Technologies). pDCs were purified by negative selection using the Human Plasmacytoid DC Enrichment Kit (STEMCELL Technologies). Cells were cultured in RPMI 1640 (Gibco) containing 10% fetal bovine serum (Gibco). After purification, purity of pDCs was higher than 90%.

For experiments on MoDCs, monocytes were isolated from PBMCs using CD14 MicroBeads (Miltenyi Biotec). Usual purity was >95% $CD14^+$. Human MoDCs were generated by incubating purified monocytes in Iscove's Modified Dulbecco's Medium (IMDM) supplemented with 10% fetal calf serum (FCS), 2 mM L-glutamine, penicillin (100 IU/ml), streptomycin (100 μg/ml), 10 mM Hepes, 1% non-essential amino acids, 1 mM sodium pyruvate, and cytokines GM-CSF (granulocyte-macrophage colony-stimulating factor) (500 IU/ml) and IL-4 (interleukin-4) (500 IU/ml) (both from Miltenyi Biotec). The obtained immature MoDCs were harvested at days 5 and 6 and phenotyped by flow cytometry before experimental use.

RNA silencing

All siRNAs were purchased from Dharmacon as pools of four individual siRNAs (ON-TARGETplus SMARTpool). Transfections of pDCs with siRNA were performed using DOTAP (Sigma-Aldrich), as previously described (*17*). Transfections of siRNA into HEK293T cells were performed using HiPerFect Transfection Reagent (Qiagen), according to the manufacturer's instructions. Transfection of MoDCs with siRNA was performed using INTERFERin (Polyplus-transfection), according to the manufacturer's recommendations.

Quantification of secreted IFN

Total IFN secreted by pDCs was titrated on STING-37 reporter cells, which correspond to HEK293 cells stably expressing an IFN-stimulated response element (ISRE)–luciferase reporter gene (*54*). A standard curve was established by applying known titers of recombinant human IFN-α2a (R&D Systems) onto STING-37 cells. Luciferase induction in STING-37 cells was determined using the Bright-Glo reagent (Promega), according to the manufacturer's recommendations. Quantification of individual IFN subtypes (IFN-α2, IFN-β, IFN-γ, IFN-λ1, and IFN-λ2/3) was performed using the LEGENDplex Kit from BioLegend (human antivirus response panel), according to the manufacturer's recommendations.

Cell culture and transfections

HEK293T cells were obtained from the American Type Culture Collection. HEK293T and STING-37 cells were cultured at 37°C and 5% CO_2 in Dulbecco's modified Eagle's medium containing 10% FCS, supplemented with 1% penicillin-streptomycin (Thermo Fisher Scientific). Transient plasmid transfections were performed using FuGENE 6 (Promega), following the manufacturer's instructions.

Immunofluorescence

Purified pDCs were washed in ice-cold 0.2% phosphate-buffered saline–bovine serum albumin (PBS-BSA), plated on poly-D-lysine–coated

slides, and fixed with 4% paraformaldehyde. Cells were permeabilized with 90% ice-cold methanol for 5 min at −20°C and, after washing, incubated with Alexa Fluor 488 mouse anti-IRF7 (pS477/pS479) and rabbit anti-TRIM8 antibody in saturation buffer PBS-BSA (0.5%) for 1 hour. Cells were then washed in saturation buffer and incubated with secondary antibody anti-mouse–AF488 and anti-rabbit–AF546 for 30 min at 4°C. Last, slides were washed in PBS and mounted in Fluoromount-G with 4′,6-diamidino-2-phenylindole (DAPI) medium (Thermo Fisher Scientific). Images were acquired using a Zeiss LSM 710 confocal microscope equipped with a PL APO 63×/1.4 oil objective. All analyses were performed using the ImageJ software (National Institutes of Health, Bethesda, MD, USA). Mander's coefficients were calculated using the JACoP plug-in in ImageJ.

RT-qPCR profiling

We designed custom RT^2 Profiler PCR arrays (Qiagen) to quantify simultaneously the expression of 75 human TRIM genes, 33 control genes (including IFNs, known ISGs, cytokines, and chemokines), and 6 housekeeping genes. The complete list of the 114 screened transcripts is shown in Table 1.

Briefly, total RNA from pDCs isolated from three blood donors and incubated or not for 16 hours with either HIV-1 or IAV was reverse-transcribed using the RT^2 First Strand Kit (Qiagen). PCRs were performed using the RT^2 Realtime SYBR Green qPCR Mastermix (Qiagen), following the manufacturer's instructions on a LightCycler 480 instrument (Roche Diagnostics). Relative expression of each target transcript was normalized to the geometric mean of the six housekeeping genes (*SDHA*, *PPIB*, *TBP*, *POLR2A*, *PPIA*, and *B2M*) and following the $2^{-\Delta\Delta Ct}$ method.

Other RT-qPCR analyses

Total RNA was extracted using an RNeasy Micro kit and submitted to deoxyribonuclease (DNase) treatment (Qiagen), following the manufacturer's instructions. RNA concentration and purity were evaluated by spectrophotometry (NanoDrop 2000c, Thermo Fisher Scientific). RNA (500 ng) was reverse-transcribed with both oligo dT and random primers using the PrimeScript RT Reagent Kit (Perfect Real Time, Takara) in a 10-µl reaction. Real-time PCRs were performed in duplicate using Takyon Rox SYBR MasterMix dTTP Blue (Eurogentec) on an Applied Biosystems QuantStudio 5 instrument. Transcripts were quantified using the following program: 3 min at 95°C followed by 35 cycles of 15 s at 95°C, 20 s at 60°C, and 20 s at 72°C. Values for each transcript were normalized to expression levels of RPL13A (60*S* ribosomal protein L13a) using the $2^{-\Delta\Delta Ct}$ method. Primers used for quantification of transcripts by real-time qPCR were indicated as follows: RPL13A, 5′-AACAGCTCATGAGGCTACGG-3′ (forward) and 5′-TGGGTCTTGAGGACCTCTGT-3′ (reverse); IFN-α2, 5′-CTTGACTTGCAGCTGAGCAC-3′ (forward) and 5′- GCTCACCCATTTCAACCAGT-3′ (reverse); IFN-β, 5′-TGCTCTCCTGTTGTGCTTCTC-3′ (forward) and 5′-CAAGCCTCCCATTCAATTGCC-3′ (reverse); TRIM8, 5′-CTGCCGTGCAAACACAACTTC-3′ (forward) and 5′-TCCACGATGTTGGTGAGCTTC-3′ (reverse); Pin1, 5′-GAGAAGATCACCCGGACCAA-3′ (forward) and 5′-AAAGTCCTCCTCTCCCGACT-3′ (reverse).

RT-qPCR in zebrafish: Each point in Fig. 7 (D and H) corresponds to an individual larva. Expression levels of each transcript were normalized to expression levels of Ef1a. The following primer sequences were used, as previously described in (*32*): Ef1a, 5′-GCTGATCGTTGGAGTCAACA-3′ (forward) and 5′-ACAGACTTGACCTCAGTGGT-3′ (reverse); Ifnphi1 (secreted isoform), 5′-TGAGAACTCAAATGTGGACCT-3′ (forward) and 5′-GTCCTCCACCTTTGACTTGT-3′ (reverse); Ifnphi3, 5′-GAGGATCAGGTTACTGGTGT-3′ (forward) and 5′-GTTCATGATGCATGTGCTGTA-3′ (reverse); CHIKV-E1 (degenerate to be indifferent to silent mutations), 5′-AARTGYGCNGTNCAVTCNATG-3′ (forward) and 5′-CCNCCNGTDATYTTYTGNACCCA-3′ (reverse).

Flow cytometry

For surface staining of BDCA-4 and CD123, pDCs were washed with PBS and incubated for 30 min at 4°C with a viability stain (Zombie Aqua Fixable Viability Kit, BioLegend). Cells were washed with magnetic-activated cell sorting (MACS) buffer (PBS, 2% fetal bovine serum, and 2 mM EDTA) and incubated for 30 min at 4°C with the appropriate antibodies or with the corresponding isotype control antibodies (5 mg/ml each) in MACS buffer containing Fc receptor blockers (BD Biosciences, San Jose, CA).

For intracellular IFN staining, cells were treated with brefeldin A (BFA) at 1 µg/ml for the last 12 hours. Cells were fixed using 2% paraformaldehyde for 10 min at room temperature. After washing the cells with MACS buffer containing 0.1% saponin (Sigma-Aldrich), cells were stained for 1 hour at 4°C in MACS buffer containing 0.1% saponin.

For intranuclear pIRF7 staining, cells were fixed with Fix Buffer I and permeabilized with Perm Buffer III (BD Biosciences), following the manufacturer's instructions. After washing the cells with MACS buffer, cells were stained for 1 hour at 4°C.

Flow cytometry analyses were performed on a BD FACSCanto II flow cytometer using flow cytometry (Diva software, BD Biosciences, San Jose, CA). FlowJo software (Tree Star, Ashland, OR) was used to analyze data.

Generation of transgenic MXA reporter zebrafish

The zebrafish *MXA* promoter used to drive the specific expression of membrane-targeted mCherry in cells responding to type I IFN signaling was amplified using the upstream primer zMXAP1 (5′-CTAAGATCGAAGCCATCAAGCA-3′) and the zMXAE1N primer matching the start codon of the MXA gene (5′-ATAAGCGGCCGCTCTCCATCCTTAATAATGTCCAA-3′). The 4.4-kb amplified fragment was digested by Not I and ligated to the coding phase of the farnesylated mCherry protein so that the MXA AUG is in phase with the downstream mCherry-F open reading frame on a I-Sce I meganuclease and Tol2-derived vector pTol2crystDsRedBNmCF, which includes an α-crystallin promoter-driven DsRed transgene to facilitate identification of transgene carriers. The resulting plasmid was injected, together with I-Sce I meganuclease (*55*), into embryos at the one-cell stage. Three independent transgenic lines from distinct founders were selected on the basis of red fluorescent protein (RFP) expression in lenses. When injected with recombinant zebrafish type I IFN (IFNϕ1), all three lines responded in a dose-dependent manner with a similar, gut-preponderant pattern of mCherry expression, although one line displayed a distinctly mosaic expression even at the F2 generation (not shown). We selected the line with the strongest homogeneous reporter expression for further studies to obtain the TG(cryaa:DsRed/MXA:mCherry-F)^{ump7} transgenic line.

Generation of *ifnphi3* mutant zebrafish

The first exon of the *ifnphi3* gene was edited using CRISPR technology. A guide RNA targeting the sequence TGGACCTTCACCGTGTGGCC(TGG) and recombinant CAS9 protein (both from TACGene, France)

were coinjected in one-cell stage eggs of wt AB zebrafish. F0 animals were raised to adulthood and backcrossed to AB. One F0 founder was found to transmit a mutated allele of *ifnphi3* in which the sequence tcaga(ATG)GACCTTCACCGTGTGG, encompassing the predicted start codon of *ifnphi3* (in parenthesis), was replaced with ATT. This results in the loss of the first 31 amino acids of the predicted protein, including its leader peptide and the first cysteine involved in a disulfide bridge key for the cytokine structure (*56*). One F1 fish bearing this allele, designated *ifnphi3*^{ip7}, was backcrossed to AB, and heterozygous F2 males and females were incrossed to generate homozygous *ifnphi3*$^{ip7/ip7}$ F3 fish. These developed normally and grew in viable and fertile adults. F4 *ifnphi3*$^{ip7/ip7}$ mutants were used to produce the eggs used in that study.

Production and infection of trim8 knockdown larvae

We followed previously described methods (*57*). Briefly, MXA reporter adults were outcrossed with wt AB zebrafish and eggs were injected at the one-cell stage with 1 nl of a 0.5 mM solution of MO (Gene Tools), targeting a trim8a or trim8b splice site (fig. S2) or a control MO with no known target. Eggs were then bleached and incubated in Volvic water at 24° or 28°C, according to the desired speed of development. One day later, 0.003% 1-phenyl-2-thiourea (Sigma-Aldrich) was added to prevent pigmentation; this was kept for all further steps. When the larvae had reached the 3-dpf stage, they were dechorionated if needed, anesthetized with tricaine (Sigma-Aldrich, A-5040), and inoculated intravenously by targeting the large vessels caudal to the cloaca, with ~200 PFU of CHIKV-GFP, as described in (*32*). After a rinse, these larvae were maintained at 28°C in individual wells of a 24-well plate and inspected at least daily with a stereomicroscope. Quantitative assessment of the clinical status, performed 3 days after inoculation, was based on a precise list of criteria, as previously described (*32*). Briefly, clinical signs were assessed blindly, yielding a disease score ranging from 0 (no disease sign) to 15 (dead or terminally ill). The signs evaluated included the following: ability to maintain equilibrium, response to touch, body shape, blood flow, cardiac rhythm, presence of edema, inflation of the swim bladder, and opacity of the yolk.

Quantitative fluorescence imaging of zebrafish

MXA reporter: 2 days after virus inoculation, anesthetized larvae were positioned laterally, left flank toward the objective, and imaged with an EVOS FL Auto microscope (Thermo Fisher Scientific) using a 2× planachromatic objective (numerical aperture, 0.06), allowing capture of the entire larva in a field. Transmitted light and fluorescence (Texas red cube) images were taken. They were further processed (superposition of channels, rotation, crop, and fluorescence intensity measure) using Fiji. A rectangular region of interest (ROI) encompassing all body regions posterior to the eyes was defined to measure transgene-associated fluorescence. CHIKV-GFP infection: 3 days after virus inoculation, larvae were mounted as above and imaged with EVOS using transmitted light and GFP fluorescence cubes and processed as described above. The percentage of GFP-positive pixels was determined with Fiji by setting a threshold of intensity yielding <0.02% positive pixels in uninfected controls.

SUPPLEMENTARY MATERIALS

Supplementary material for this article is available at http://advances.sciencemag.org/cgi/content/full/5/11/eaax3511/DC1

Fig. S1. TRIM expression and silencing in human primary pDCs.

Fig. S2. Verification of knockdown efficiency in zebrafish.

View/request a protocol for this paper from *Bio-protocol*.

REFERENCES AND NOTES

1. S. Akira, S. Uematsu, O. Takeuchi, Pathogen recognition and innate immunity. *Cell* **124**, 783–801 (2006).
2. K. Honda, H. Yanai, H. Negishi, M. Asagiri, M. Sato, T. Mizutani, N. Shimada, Y. Ohba, A. Takaoka, N. Yoshida, T. Taniguchi, IRF-7 is the master regulator of type-I interferon-dependent immune responses. *Nature* **434**, 772–777 (2005).
3. Y. J. Liu, IPC: Professional type 1 interferon-producing cells and plasmacytoid dendritic cell precursors. *Annu. Rev. Immunol.* **23**, 275–306 (2005).
4. A. L. Blasius, B. Beutler, Intracellular toll-like receptors. *Immunity* **32**, 305–315 (2010).
5. X. Dagenais-Lussier, H. Loucif, A. Murira, X. Laulhe, S. Stager, A. Lamarre, J. van Grevenynghe, Sustained IFN-I expression during established persistent viral infection: A "bad seed" for protective immunity. *Viruses* **10**, (2017).
6. G. Trinchieri, Type I interferon: Friend or foe? *J. Exp. Med.* **207**, 2053–2063 (2010).
7. S. Nisole, J. P. Stoye, A. Saib, TRIM family proteins: Retroviral restriction and antiviral defence. *Nat. Rev. Microbiol.* **3**, 799–808 (2005).
8. A. Reymond, G. Meroni, A. Fantozzi, G. Merla, S. Cairo, L. Luzi, D. Riganelli, E. Zanaria, S. Messali, S. Cainarca, A. Guffanti, S. Minucci, P. G. Pelicci, A. Ballabio, The tripartite motif family identifies cell compartments. *EMBO J.* **20**, 2140–2151 (2001).
9. M. van Gent, K. M. J. Sparrer, M. U. Gack, TRIM proteins and their roles in antiviral host defenses. *Annu. Rev. Virol.* **5**, 385–405 (2018).
10. G. A. Versteeg, S. Benke, A. Garcia-Sastre, R. Rajsbaum, InTRIMsic immunity: Positive and negative regulation of immune signaling by tripartite motif proteins. *Cytokine Growth Factor Rev.* **25**, 563–576 (2014).
11. G. A. Versteeg, R. Rajsbaum, M. T. Sanchez-Aparicio, A. M. Maestre, J. Valdiviezo, M. Shi, K. S. Inn, A. Fernandez-Sesma, J. Jung, A. Garcia-Sastre, The E3-ligase TRIM family of proteins regulates signaling pathways triggered by innate immune pattern-recognition receptors. *Immunity* **38**, 384–398 (2013).
12. F. W. McNab, R. Rajsbaum, J. P. Stoye, A. O'Garra, Tripartite-motif proteins and innate immune regulation. *Curr. Opin. Immunol.* **23**, 46–56 (2011).
13. A. S. Beignon, K. McKenna, M. Skoberne, O. Manches, I. DaSilva, D. G. Kavanagh, M. Larsson, R. J. Gorelick, J. D. Lifson, N. Bhardwaj, Endocytosis of HIV-1 activates plasmacytoid dendritic cells via Toll-like receptor-viral RNA interactions. *J. Clin. Invest.* **115**, 3265–3275 (2005).
14. S. S. Diebold, T. Kaisho, H. Hemmi, S. Akira, C. Reis e Sousa, Innate antiviral responses by means of TLR7-mediated recognition of single-stranded RNA. *Science* **303**, 1529–1531 (2004).
15. J. A. Young, D. Sermwittayawong, H. J. Kim, S. Nandu, N. An, H. Erdjument-Bromage, P. Tempst, L. Coscoy, A. Winoto, Fas-associated death domain (FADD) and the E3 ubiquitin-protein ligase TRIM21 interact to negatively regulate virus-induced interferon production. *J. Biol. Chem.* **286**, 6521–6531 (2011).
16. W. Zhao, L. Wang, M. Zhang, P. Wang, C. Yuan, J. Qi, H. Meng, C. Gao, Tripartite motif-containing protein 38 negatively regulates TLR3/4- and RIG-I-mediated IFN-beta production and antiviral response by targeting NAP1. *J. Immunol.* **188**, 5311–5318 (2012).
17. N. Smith, P. O. Vidalain, S. Nisole, J. P. Herbeuval, An efficient method for gene silencing in human primary plasmacytoid dendritic cells: Silencing of the TLR7/IRF-7 pathway as a proof of concept. *Sci. Rep.* **6**, 29891 (2016).
18. S. Ning, J. S. Pagano, G. N. Barber, IRF7: Activation, regulation, modification and function. *Genes Immun.* **12**, 399–414 (2011).
19. M. Sato, N. Hata, M. Asagiri, T. Nakaya, T. Taniguchi, N. Tanaka, Positive feedback regulation of type I IFN genes by the IFN-inducible transcription factor IRF-7. *FEBS Lett.* **441**, 106–110 (1998).
20. L. Strahle, D. Garcin, D. Kolakofsky, Sendai virus defective-interfering genomes and the activation of interferon-beta. *Virology* **351**, 101–111 (2006).
21. R. Lin, Y. Mamane, J. Hiscott, Multiple regulatory domains control IRF-7 activity in response to virus infection. *J. Biol. Chem.* **275**, 34320–34327 (2000).
22. D. Komander, M. Rape, The ubiquitin code. *Annu. Rev. Biochem.* **81**, 203–229 (2012).
23. K. N. Swatek, D. Komander, Ubiquitin modifications. *Cell Res.* **26**, 399–422 (2016).
24. K. Yang, H. X. Shi, X. Y. Liu, Y. F. Shan, B. Wei, S. Chen, C. Wang, TRIM21 is essential to sustain IFN regulatory factor 3 activation during antiviral response. *J. Immunol.* **182**, 3782–3792 (2009).
25. F. El Asmi, M. A. Maroui, J. Dutrieux, D. Blondel, S. Nisole, M. K. Chelbi-Alix, Implication of PMLIV in both intrinsic and innate immunity. *PLoS Pathog.* **10**, e1003975 (2014).
26. T. Saitoh, A. Tun-Kyi, A. Ryo, M. Yamamoto, G. Finn, T. Fujita, S. Akira, N. Yamamoto, K. P. Lu, S. Yamaoka, Negative regulation of interferon-regulatory factor 3-dependent innate antiviral response by the prolyl isomerase Pin1. *Nat. Immunol.* **7**, 598–605 (2006).
27. Y. C. Liou, X. Z. Zhou, K. P. Lu, Prolyl isomerase Pin1 as a molecular switch to determine the fate of phosphoproteins. *Trends Biochem. Sci.* **36**, 501–514 (2011).
28. V. Briolat, L. Jouneau, R. Carvalho, N. Palha, C. Langevin, P. Herbomel, O. Schwartz, H. P. Spaink, J. P. Levraud, P. Boudinot, Contrasted innate responses to two viruses in zebrafish: Insights into the ancestral repertoire of vertebrate IFN-stimulated genes. *J. Immunol.* **192**, 4328–4341 (2014).

29. P. Boudinot, C. Langevin, C. J. Secombes, J. P. Levraud, The peculiar characteristics of fish type I interferons. *Viruses* **8**, e298 (2016).
30. M. S. Ibarra, C. Borini Etichetti, C. Di Benedetto, G. L. Rosano, E. Margarit, G. Del Sal, M. Mione, J. Girardini, Dynamic regulation of Pin1 expression and function during zebrafish development. *PLoS ONE* **12**, e0175939 (2017).
31. L. Micale, M.N. Loviglio, M. Manzoni, C. Fusco, B. Augello, E. Migliavacca, G. Cotugno, E. Monti, G. Borsani, A. Reymond, G. Merla, A fish-specific transposable element shapes the repertoire of p53 target genes in zebrafish. *PLoS ONE* **7**, e46642 (2012).
32. N. Palha, F. Guivel-Benhassine, V. Briolat, G. Lutfalla, M. Sourisseau, F. Ellett, C. H. Wang, G. J. Lieschke, P. Herbomel, O. Schwartz, J. P. Levraud, Real-time whole-body visualization of chikungunya virus infection and host interferon response in zebrafish. *PLoS Pathog.* **9**, e1003619 (2013).
33. L. Carthagena, A. Bergamaschi, J. M. Luna, A. David, P. D. Uchil, F. Margottin-Goguet, W. Mothes, U. Hazan, C. Transy, G. Pancino, S. Nisole, Human TRIM gene expression in response to interferons. *PLoS ONE* **4**, e4894 (2009).
34. R. Rajsbaum, J. P. Stoye, A. O'Garra, Type I interferon-dependent and -independent expression of tripartite motif proteins in immune cells. *Eur. J. Immunol.* **38**, 619–630 (2008).
35. Q. Liang, H. Deng, X. Li, X. Wu, Q. Tang, T. H. Chang, H. Peng, F. J. Rauscher III, K. Ozato, F. Zhu, Tripartite motif-containing protein 28 is a small ubiquitin-related modifier E3 ligase and negative regulator of IFN regulatory factor 7. *J. Immunol.* **187**, 4754–4763 (2011).
36. M. U. Gack, Y. C. Shin, C. H. Joo, T. Urano, C. Liang, L. Sun, O. Takeuchi, S. Akira, Z. Chen, S. Inoue, J. U. Jung, TRIM25 RING-finger E3 ubiquitin ligase is essential for RIG-I-mediated antiviral activity. *Nature* **446**, 916–920 (2007).
37. S. R. Vincent, D. A. Kwasnicka, P. Fretier, A novel RING finger-B box-coiled-coil protein, GERP. *Biochem. Biophys. Res. Commun.* **279**, 482–486 (2000).
38. M. F. Caratozzolo, F. Marzano, F. Mastropasqua, E. Sbisa, A. Tullo, TRIM8: Making the right decision between the oncogene and tumour suppressor role. *Genes* **8**, 354 (2017).
39. M. F. Caratozzolo, L. Micale, M. G. Turturo, S. Cornacchia, C. Fusco, F. Marzano, B. Augello, A. M. D'Erchia, L. Guerrini, G. Pesole, E. Sbisa, G. Merla, A. Tullo, TRIM8 modulates p53 activity to dictate cell cycle arrest. *Cell Cycle* **11**, 511–523 (2012).
40. D. Tomar, L. Sripada, P. Prajapati, R. Singh, A. K. Singh, R. Singh, Nucleo-cytoplasmic trafficking of TRIM8, a novel oncogene, is involved in positive regulation of TNF induced NF-kappaB pathway. *PLoS ONE* **7**, e48662 (2012).
41. Q. Li, J. Yan, A. P. Mao, C. Li, Y. Ran, H. B. Shu, Y. Wang, Tripartite motif 8 (TRIM8) modulates TNFalpha- and IL-1beta-triggered NF-kappaB activation by targeting TAK1 for K63-linked polyubiquitination. *Proc. Natl. Acad. Sci. U.S.A.* **108**, 19341–19346 (2011).
42. E. Toniato, X. P. Chen, J. Losman, V. Flati, L. Donahue, P. Rothman, TRIM8/GERP RING finger protein interacts with SOCS-1. *J. Biol. Chem.* **277**, 37315–37322 (2002).
43. F. Okumura, Y. Matsunaga, Y. Katayama, K. I. Nakayama, S. Hatakeyama, TRIM8 modulates STAT3 activity through negative regulation of PIAS3. *J. Cell Sci.* **123**, 2238–2245 (2010).
44. W. Ye, M. M. Hu, C. Q. Lei, Q. Zhou, H. Lin, M. S. Sun, H. B. Shu, TRIM8 negatively regulates TLR3/4-mediated innate immune response by blocking TRIF-TBK1 interaction. *J. Immunol.* **199**, 1856–1864 (2017).
45. Y. Huang, Y. Yu, Y. Yang, M. Yang, L. Zhou, X. Huang, Q. Qin, Fish TRIM8 exerts antiviral roles through regulation of the proinflammatory factors and interferon signaling. *Fish Shellfish Immunol.* **54**, 435–444 (2016).
46. R. Rajsbaum, A. Garcia-Sastre, G. A. Versteeg, TRIMmunity: The roles of the TRIM E3-ubiquitin ligase family in innate antiviral immunity. *J. Mol. Biol.* **426**, 1265–1284 (2014).
47. R. Higgs, E. Lazzari, C. Wynne, J. Ni Gabhann, A. Espinosa, M. Wahren-Herlenius, C. A. Jefferies, Self protection from anti-viral responses—Ro52 promotes degradation of the transcription factor IRF7 downstream of the viral Toll-Like receptors. *PLoS ONE* **5**, e11776 (2010).
48. R. Higgs, J. Ni Gabhann, N. Ben Larbi, E. P. Breen, K. A. Fitzgerald, C. A. Jefferies, The E3 ubiquitin ligase Ro52 negatively regulates IFN-beta production post-pathogen recognition by polyubiquitin-mediated degradation of IRF3. *J. Immunol.* **181**, 1780–1786 (2008).
49. M. Sato, H. Suemori, N. Hata, M. Asagiri, K. Ogasawara, K. Nakao, T. Nakaya, M. Katsuki, S. Noguchi, N. Tanaka, T. Taniguchi, Distinct and essential roles of transcription factors IRF-3 and IRF-7 in response to viruses for IFN-alpha/beta gene induction. *Immunity* **13**, 539–548 (2000).
50. B. Reizis, A. Bunin, H. S. Ghosh, K. L. Lewis, V. Sisirak, Plasmacytoid dendritic cells: Recent progress and open questions. *Annu. Rev. Immunol.* **29**, 163–183 (2011).
51. K. L. Lim, K. C. Chew, J. M. Tan, C. Wang, K. K. Chung, Y. Zhang, Y. Tanaka Smith, S. Engelender, C. A. Ross, V. L. Dawson, T. M. Dawson, Parkin mediates nonclassical, proteasomal-independent ubiquitination of synphilin-1: Implications for Lewy body formation. *J. Neurosci.* **25**, 2002–2009 (2005).
52. J. L. Rossio, M. T. Esser, K. Suryanarayana, D. K. Schneider, J. W. Bess Jr., G. M. Vasquez, T. A. Wiltrout, E. Chertova, M. K. Grimes, Q. Sattentau, L. O. Arthur, L. E. Henderson, J. D. Lifson, Inactivation of human immunodeficiency virus type 1 infectivity with preservation of conformational and functional integrity of virion surface proteins. *J. Virol.* **72**, 7992–8001 (1998).
53. T. Doyle, O. Moncorge, B. Bonaventure, D. Pollpeter, M. Lussignol, M. Tauziet, L. Apolonia, M. T. Catanese, C. Goujon, M. H. Malim, The interferon-inducible isoform of NCOA7 inhibits endosome-mediated viral entry. *Nat. Microbiol.* **3**, 1369–1376 (2018).
54. M. Lucas-Hourani, D. Dauzonne, P. Jorda, G. Cousin, A. Lupan, O. Helynck, G. Caignard, G. Janvier, G. Andre-Leroux, S. Khiar, N. Escriou, P. Despres, Y. Jacob, H. Munier-Lehmann, F. Tangy, P. O. Vidalain, Inhibition of pyrimidine biosynthesis pathway suppresses viral growth through innate immunity. *PLoS Pathog.* **9**, e1003678 (2013).
55. V. Thermes, C. Grabher, F. Ristoratore, F. Bourrat, A. Choulika, J. Wittbrodt, J. S. Joly, I-SceI meganuclease mediates highly efficient transgenesis in fish. *Mech. Dev.* **118**, 91–98.
56. J. Zou, C. Tafalla, J. Truckle, C. J. Secombes, Identification of a second group of type I IFNs in fish sheds light on IFN evolution in vertebrates. *J. Immunol.* **179**, 3859–3871 (2007).
57. J. P. Levraud, E. Colucci-Guyon, M. J. Redd, G. Lutfalla, P. Herbomel, In vivo analysis of zebrafish innate immunity. *Methods Mol. Biol.* **415**, 337–363 (2008).

Acknowledgments: We are grateful to G. Meroni, P. O. Vidalain, J. Hiscott, D. Garcin, and B. Jahrsdörfer for providing invaluable materials. Furthermore, we personally thank J. Bess and J. Lifson for providing us with the inactivated purified HIV-1 viruses. We acknowledge the imaging facility MRI, member of the national infrastructure France-BioImaging supported by the French National Research Agency (ANR-10-INBS-04, "Investissements d'avenir"). These experiments used regents provided by the AIDS and Cancer Virus Program, Biological Products Core Laboratory, Frederick National Laboratory for Cancer Research, supported with federal funds from the National Cancer Institute, NIH, under contract HHSN261200800001E. **Funding:** This work was supported by Labex EpiGenMed, an Investissements d'avenir program (ANR-10-LABX-12-01 to N.J.A. and S.N.); the Agence National de la Recherche sur le SIDA et les Hépatites virales, ANRS (AO2017-1 to J.-P.H.); the European Community's Seventh Framework Program (FP7- PEOPLE-2011-ITN) under the Marie-Curie Initial Training Network FishForPharma (PITN-GA-2011-289209 to G.L.); the European Community's H2020 Program Marie-Curie Innovative Training Network ImageInLife (721537 to G.L. and J.-P.L.); the Agence Nationale de la Recherche (ANR-16-CE20-0002-03 and ANR-10-MDI-009 to J.-P.L.); and the Région Occitanie (REPERE2017ImageInLife to G.L.). G.M. (AO2018-2), N.S. (AO2016-1), O.M. (AO2017-1), and S.M. (AO2017-2) were supported by grants from the ANRS. This work received help and expertise from TACGene, which is supported by the program Investissement d'avenir TEFOR (ANR-II-INSB-0014). N.S. acknowledges support from the European Molecular Biology Organization EMBO for Fellowship (LT-834-2017), the start-up funding program "Baustein" of the Medical Faculty of Ulm University (LSBN.0147), and the Deutsche Forschungsgemeinschaft DFG (SM 544/1-1). **Author contributions:** S.N. conceived the study. G.M., N.S., J.-P.H., J.-P.L., and S.N. designed the experiments. G.M., N.S., S.M., O.M., C.C., F.P.B., J.-P.L., N.J.A., and S.N. performed the experiments. G.M., N.S., J.-P.L., N.J.A., and S.N. analyzed and interpreted data. O.M., J.E., F.S., G.L., J.-P.L., and S.N. provided tools and expertise. N.J.A. and S.N. wrote the paper. All authors discussed the results and commented on the manuscript. **Competing interests:** The authors declare that they have no competing interests. **Data and materials availability:** All data needed to evaluate the conclusions in the paper are present in the paper and/or the Supplementary Materials. Additional data are available from authors upon request. The zebrafish lines (MXA:mCherry transgenic reporter of ifnphi3-null mutant) can be provided by Institut Pasteur pending scientific review and a completed material transfer agreement. Requests should be submitted to J.-P.L. (jean-pierre.levraud@pasteur.fr).

Submitted 15 March 2019
Accepted 20 September 2019
Published 20 November 2019
10.1126/sciadv.aax3511

Citation: G. Maarifi, N. Smith, S. Maillet, O. Moncorgé, C. Chamontin, J. Edouard, F. Sohm, F. P. Blanchet, J.-P. Herbeuval, G. Lutfalla, J.-P. Levraud, N. J. Arhel, S. Nisole, TRIM8 is required for virus-induced IFN response in human plasmacytoid dendritic cells. *Sci. Adv.* **5**, eaax3511 (2019).